CHAPTER

S15

Climate and the Oceans

This chapter on climate variability and climate change appears only on the textbook Web site http://booksite.academicpress.com/DPO/. The first section introduces climate variability and climate change. This is followed by a section on climate modes and variability for each of the ocean basins in the order of the basin chapters 9 through 13 (Atlantic, Pacific, Indian, Arctic, and Southern Ocean). The final section summarizes global ocean observations indicative of climate change. Each of the basin-oriented subsections can be read as an addendum to the print chapter for that basin.

S15.1. INTRODUCTION

S15.1.1. Definitions

Climate is variability in any part of the ocean-atmosphere-land-ecology system on timescales that are longer than seasonal. Climate variations can be due to natural, internal interactions between components of the system; to natural, external forcing; or to anthropogenic external forcing. In present-day usage, *climate variability* usually refers to natural climate variability and *climate change* refers to anthropogenically forced variations in climate. Examples of internal interactions include some of the feedbacks described in this text (i.e., the Bjerknes tropical ocean-atmosphere feedback or the ice-albedo feedback), and a plethora of others that are described in books and journals devoted to the topic of climate variations. Examples of natural external forcing include variations in the Earth-moon-Sun orbits, and random but ongoing volcanism. Examples of anthropogenic forcing include burning of fossil fuels, and changes in land surfaces due to patterns of land use; changes in these forcings can then set off feedbacks that could move the climate system to a different state. We categorize climate timescales as *interannual* (roughly longer than a year and shorter than about eight years), *decadal* (roughly one to several decades), centennial, millennial, and longer. For the shorter timescales, time series observations of the property of interest are used. For the ocean these include temperature, salinity, oxygen, nutrients, carbon parameters, current velocities, surface height, and so forth. For the longer timescales, which are the realm of paleoclimate studies, "proxy" records of something that depends on the property of interest are used such as the prevalence of different types of benthic foraminifera or the size of a tree ring, which can be related to changes in temperature, precipitation, and so on.

Most of this text is concerned with the mean structure of the ocean circulation and properties, and for some regions, its seasonal variability. Climate is included in this descriptive oceanography text because it affects ocean

variability in properties and circulation on timescales of years to millennia. Climate variability and climate change usually result in small changes, of the order of 10%, in the mean structures. The most energetic modes of variability, which are the tropical modes such as El Niño-Southern Oscillation, result in much larger changes in the structure, but even these do not eliminate the mean pycnocline or vertical temperature structure.

As another example, no climate variability or change would ever remove the importance of western boundary currents, because their existence is due to Earth's rotation and the presence of ocean boundaries, neither of which will vanish although the boundaries do change on geological timescales. Moreover, Earth will continue to be heated in the tropics and cooled at high latitudes, and the organization of the major wind systems is unlikely to change. (These include the easterly and westerly winds associated with the Hadley, Ferrel, and Polar cells, and the tropical circulations such as the Walker circulation and monsoons.) Climate variations are therefore unlikely to cause the demise or complete reorganization of the Gulf Stream or any of the other western boundary currents. The strength might change, the position of the separated currents might shift somewhat, and the advected properties might be somewhat altered, but the basic structure would remain as long as the general surface wind forcing patterns exist.

On the other hand, major changes in ocean stratification due to heating, precipitation and evaporation, and sea ice could change the strength and structure of the overturning circulation. Such changes are apparent in paleoclimate records such as the production and properties of North Atlantic Deep Water were vastly altered during the last glaciation. Changes in stratification in the tropics could alter the El Niño-Southern Oscillation (ENSO) feedbacks, with a warmer, more stratified ocean much less capable of producing the cold tongue of the eastern tropical Pacific. Since ENSO affects temperature and precipitation over a large part of the globe, such changes could have widespread consequences.

S15.1.2. Natural Modes of Climate Variability

In each of the subsequent sections focused on each ocean basin, some of the most energetic (natural) modes of interannual and decadal climate variability are described. These are summarized in Table S15.1. Each mode has been described in terms of an index that can be calculated and plotted over many decades. Correlations of surface temperature and sea level pressure with many of the indices are shown in later sections and are listed in the table.

Climate modes with dominantly interannual variability are (a) the El Niño-Southern Oscillation (ENSO), (b) the Atlantic Meridional Mode (AMM), Atlantic Niño, and (c) the Indian Ocean Dipole (IOD) mode. These are all tropical modes of variability with their relatively high frequency set by tropical dynamics; all of these modes include strong feedback between the atmosphere and ocean. ENSO is the most energetic of these globally by far, with a sea level pressure pattern that includes the central-eastern tropical Pacific (one sign), western tropical Pacific and eastern Indian Ocean (opposite sign), and the tropical Atlantic (opposite sign), with a signature over North America and in the western tropical Atlantic (Figure 10.28 and Section S15.2.1). The intrinsic Atlantic and Indian interannual modes are mostly confined within their own ocean basins.

Climate modes with dominantly decadal variability are (a) the North Atlantic Oscillation (NAO) and closely related Arctic Oscillation (AO or Northern Annular Mode, NAM), (b) the Antarctic Oscillation (AAO or Southern Annular Mode, SAM), and (c) the Pacific Decadal Oscillation (PDO) with its closely related modes that are defined within the North

TABLE S15.1 Some of the Principal Modes of Natural Climate Variability

Climate Mode	Acronym	Approximate Timescale	Section and Map
Atlantic Meridional Mode	AMM	Interannual	Sections S15.2.1 and S15.5, Figure S15.1
Atlantic Niño	—	Interannual	Section S15.2.1, Figure S15.1
Arctic Oscillation (also called Northern Annular Mode) and the closely related North Atlantic Oscillation	AO (NAM) NAO	Decadal	Sections S15.2.2 and S15.5, Figure S15.2
East Atlantic Pattern	EAP	Decadal	Section S15.2.2, Figure S15.2
Atlantic Multidecadal Oscillation	AMO	Multidecadal	Section S15.2.2, Figure S15.2 Section S15.5
El Niño-Southern Oscillation (Southern Oscillation Index)	ENSO (SOI)	Interannual	Section 10.8, Figure 10.28
Pacific Decadal Oscillation (closely related: North Pacific Index and Pacific North American teleconnection)	PDO (NPI) (PNA)	Decadal	Section S15.3, Figure S15.5
North Pacific Gyre Oscillation	NPGO	Decadal	Section S15.3, Figure S15.6
Indian Ocean Dipole mode	IOD	Interannual	Section S15.4
Antarctic Oscillation (also called the Southern Annular Mode)	AAO (SAM)	Decadal	Section S15.6, Figure S15.15

Pacific. These modes do not tend to have strong, obvious feedbacks between the ocean and atmosphere, although much work has been done and continues to be done on such mechanisms.

The only centennial mode described herein and listed in Table S15.1 is the AMO, which is defined in terms of basin-wide sea-surface temperature (SST) averages and is presumed to be linked to variations in the meridional overturning circulation (MOC). The AMO also affects the Arctic Ocean.

The AAO (SAM) and the PDO have similar spatial patterns, and both have similarities with the interannual ENSO pattern. That is, all three have strongest signatures in the Pacific, Indian, and Antarctic, as if the Pacific region is connected primarily zonally to the Indian and meridionally to the Antarctic. There is little correlation with the Arctic. The NAO (AO) pattern, on the other hand, connects the Atlantic Ocean meridionally with the Arctic with little signature in the Southern Hemisphere, even in the tropical Atlantic.

These modes of climate variability are described in subsequent sections as simply as possible, as if they were standing patterns, with the oceans and land determining to some extent the location of the nodes. Many of the modes are also analyzed in terms of lagged correlations and large-scale wavelike propagation, but this is beyond the scope of this text.

These natural modes of climate variability not only have importance for regional climate variation in the ocean, but are also the natural modes of the entire system that could be forced anthropogenically. Shifts into a particular phase of modes such as ENSO, the PDO, SAM, and NAO/AO are sometimes suggested by climate

prediction models. As we begin to consider consequences of continuing changes in greenhouse gases, particulates in the atmosphere, and land use, some of the hypotheses naturally involve projection of climate change forcing on these climate modes.

S15.2. CLIMATE AND THE ATLANTIC OCEAN

Atlantic climate research tends to be focused on decadal and longer term variability centered on the northern North Atlantic's deep-water formation processes and on sea ice processes in the Nordic Seas and Arctic (Section S15.5). This is because the mean ventilation age of northern North Atlantic deep waters is on the order of decades or less with associated measurable variability. However, climate variability at all timescales from interannual to decadal, centennial, and millennial has been documented and affects all regions of the Atlantic (Table S15.1). Trends that have been related to climate change (anthropogenic forcing) have also been documented.

S15.2.1. Tropical Atlantic Variability

Interannual variability studies are focused on the tropical Atlantic, where there are several modes, including two intrinsic to the Atlantic. These are (1) the *Atlantic Meridional Mode* (AMM), which is a cross-equatorial mode; (2) the *Atlantic Niño*, which is a zonal equatorial mode that is dynamically similar to ENSO with a tropical Bjerknes feedback (Section 7.9.2); and (3) remote forcing from the Pacific ENSO. None of these modes is overwhelmingly dominant in the sense of the Pacific's ENSO. Variability in the upper ocean is linked to these modes. Variability at intermediate and abyssal depths may have other sources and timescales. Tropical Atlantic variability is regularly monitored with the PIRATA array (Section S16.5.6.2 and Figure S16.38), which was designed to sample both the meridional and zonal modes (Bourlès et al., 2008).

AMM has SST anomalies of opposite sign on either side of the equator: warm SST to the north and cold SST to the south and vice versa (Figure S15.1a). Because of these opposing anomalies, the AMM is also called the "tropical dipole mode." Surface wind anomalies blow toward the warm SST. During positive AMM, the Intertropical Convergence Zone (ITCZ), which lies in the Northern Hemisphere, is displaced northward. The AMM's full Atlantic hemispheric pattern includes alternating highs and lows from the Nordic Seas to the Southern Ocean, but its amplitude is largest in the tropics, while the North Atlantic Oscillation, whose spatial pattern it resembles, has highest amplitude in the north. The AMM has a seasonal cycle, peaking in boreal spring, and interannual to decadal variability. Decadal variation in the AMM has been described in terms of a wind-evaporation-SST feedback[1] (Chang, Ji, & Li, 1997; Kushnir, Seager, Miller, & Chiang, 2002; Figure S15.1e), but the feedback is weak (Sutton, Jewson, & Rowell, 2000; Chiang &Vimont, 2004). External forcing, for instance from the NAO or Pacific's ENSO, appears to be necessary to maintain the decadal energy.

The Atlantic Niño, also known as the "Atlantic zonal equatorial mode" (Figure

[1] A feedback diagram is shown in Figure S15.1e. Starting with a positive SST dipole (warm north of the equator), the surface winds blow northwestward south of the equator and northeastward north of the equator. This decreases the easterly trade winds in the Northern Hemisphere, which reduces the evaporative heat flux in the Northern Hemisphere, since evaporative heat flux is proportional to wind speed. This enhances the SST anomaly there, hence is a positive feedback. The system is restored by a slower negative feedback involving advective heat flux in the ocean with the cooler southern waters advected northward by the North Brazil Current that is strengthened by the winds.

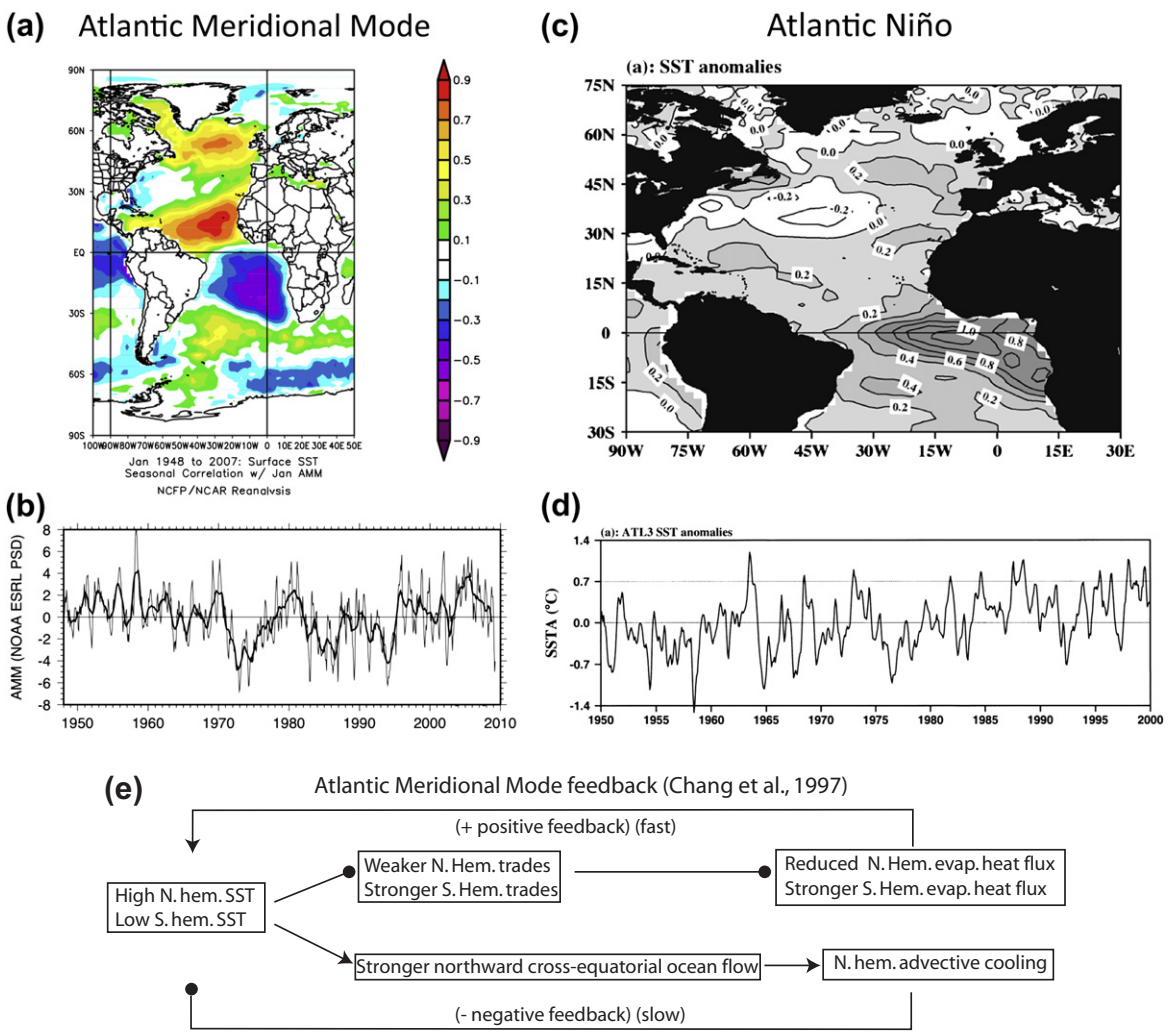

FIGURE S15.1 Tropical Atlantic interannual climate modes.(a, b) Atlantic Meridional Mode: SST correlation with the AMM index for 1948–2007, all months and monthly time series (light) of the AMM index, with a one-year running mean (heavy). (Data and graphical interface from NOAA ESRL, 2009b). (c, d) Atlantic "Niño" (zonal equatorial mode): SST anomalies and time series of temperature averaged in the cold-tongue region 3°S–3°N, 20°W–0° ("ATL3 index"). High values correspond to the Niño state (weak or absent cold tongue). ©American Meteorological Society. Reprinted with permission. *Source: From Wang (2002).* (e) Feedbacks for AMM decadal variability. Arrowheads mean an upward trend in the cause results in an upward trend in the result, circles indicate upward trend resulting in negative trend. (Based on Chang et al., 1997; Kushnir et al., 2002).

S15.1c,d) has the typical Bjerknes tropical feedback between the ocean's SST and atmosphere's winds (Section 7.9.2). The timescale of the Atlantic Niño is interannual, on the order of 30 months, but with considerable randomness. In the normal seasonal cycle, a *cold tongue* appears in the central and eastern Atlantic every boreal summer (Figure S15.1c). The seasonal cold tongue occupies a large fraction of the equatorial Atlantic, with coldest temperatures less

than 24 °C, comparable to the Pacific's seasonal cold tongue temperatures (Section 10.7.3). The western *warm pool* in the Atlantic, at about 28 °C, is cooler and more spatially limited than the Pacific's warm pool (>30 °C; Figure 10.25). During an Atlantic Niño, warm SST anomalies almost obliterate the cold tongue (e.g., 1998 in Figure S15.1d). This is accompanied by an eastward shift and weakening of the Atlantic's Walker circulation, with rising air over the maximum anomaly in the central Atlantic, and a strengthening of the Hadley circulation (Wang, 2002).

The Atlantic Niño has lower amplitude and a smaller geographical impact than the Pacific's ENSO. The simplest explanation is that the Atlantic is much narrower than the Pacific, so the thermocline depth variation in the east and the associated SST anomalies are weaker in the Atlantic (Jin, 1996). Since the mean western warm pool is much narrower and cooler than in the Pacific, Atlantic anomalies there are also weaker than in the Pacific.

The Pacific's ENSO reaches eastward into the tropical Atlantic (Wang, 2002). During an El Niño warm event, the Pacific's Walker circulation shifts eastward with ascending air moving to the central and eastern equatorial Pacific. The descending branch of this anomalous Walker circulation is in the central Atlantic with strongest effects on SST in the tropical North Atlantic. Tropical Atlantic SST anomalies lag a Pacific El Niño warm event by five to six months.

S15.2.2. Decadal and Multidecadal Variability

North Atlantic decadal variability is often interpreted in terms of the *North Atlantic Oscillation* (NAO) and *East Atlantic Pattern* (EAP), which are internal modes of the atmosphere at short timescales that have important decadal and longer term variability that might involve feedbacks with the ocean. The NAO is closely related to the AO (NAM) (Section S15.5). In the South Atlantic, decadal climate variability is associated with the SAM (Section S15.6). The *Atlantic Multidecadal Oscillation* (AMO) represents a longer timescale natural mode of the Atlantic overturning circulation associated with surface temperatures throughout the North Atlantic.

The NAO is one of the most vigorous and best described of Earth's natural climate modes (Hurrell, Kushnir, Ottersen, & Visbeck, 2003; Visbeck et al., 2003). In the mean, the North Atlantic's westerly winds are forced by the lower atmosphere's pressure difference between the subtropical (Bermuda) high and subpolar (Iceland) low. When the pressure systems shift or change in strength, the westerly wind location and strength also change. The traditional NAO index is the difference in pressure between Portugal and Iceland, although other indices are also used. When the NAO is positive, the pressure difference is large and the westerlies are shifted northward relative to their mean position; that is, with maximum strength between Portugal and Iceland, and vice versa. NAO variability is only roughly decadal and includes seasonal to multidecadal timescales (Figure S15.2d). A high NAO with strong westerlies, a cold subpolar gyre, and warm Nordic Seas and Gulf Stream region dominated from the 1970s to 1990s. A low NAO dominated from the 1950s to 1960s.

Shifts in the NAO affect North Atlantic circulation and the production and properties of its water masses. Associated with high NAO, the Gulf Stream and its separation point move slightly but measurably northward and transport increases, lagging the NAO by several years (Curry & McCartney, 2001; Visbeck et al., 2003). Also during high NAO, the subpolar gyre circulation north of about 50°N shifts westward and intensifies (Flatau, Talley, & Niiler, 2003; Häkkinen & Rhines, 2004). Because the North Atlantic forms intermediate and deep water, its properties are highly variable from

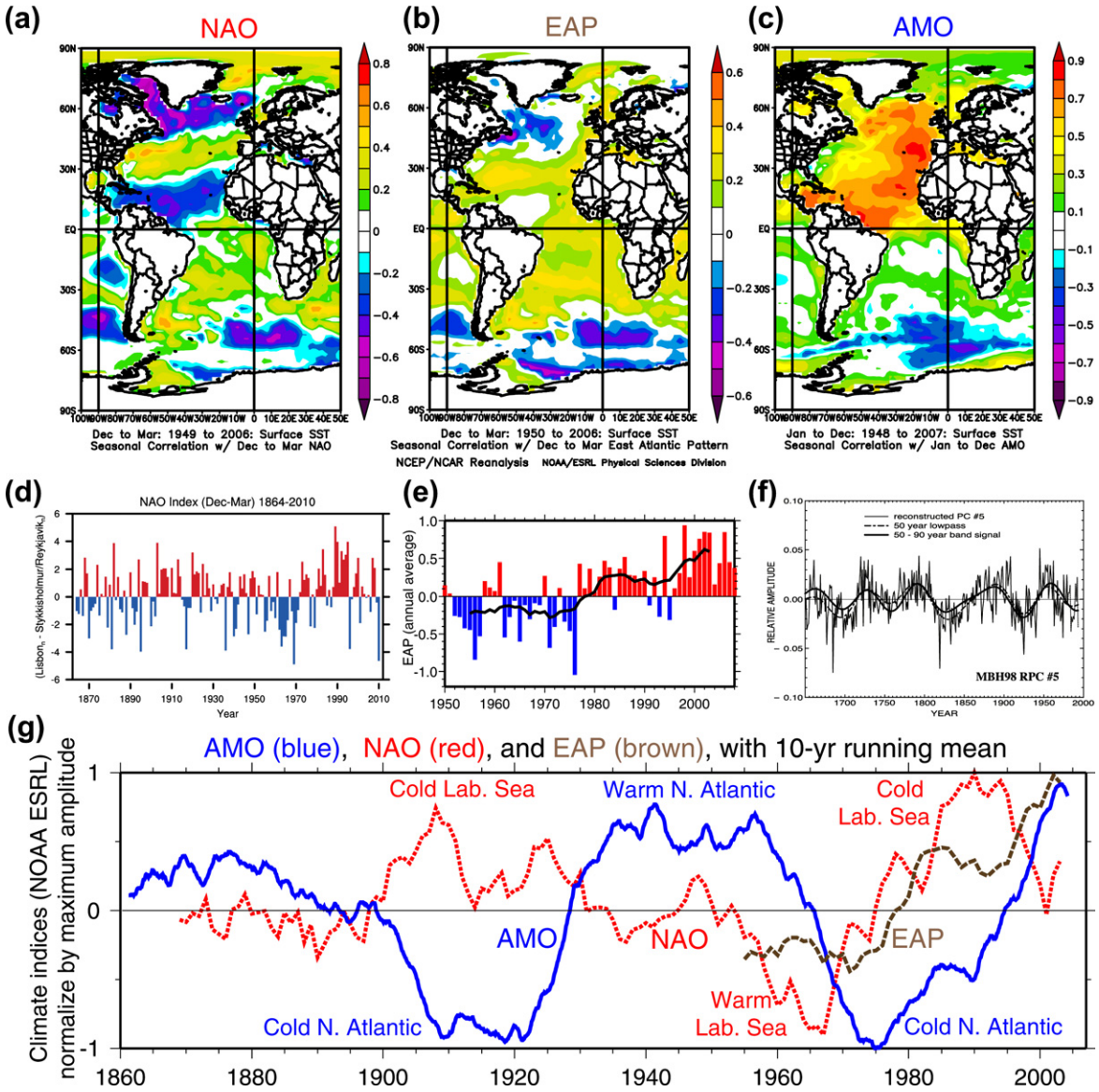

FIGURE S15.2 Atlantic decadal to multidecadal climate modes. (a) North Atlantic Oscillation (NAO), (b) East Atlantic Pattern (EAP), and (c) Atlantic Multidecadal Oscillation (AMO). Maps of SST correlation with each index: positive is warm and negative is cold. (Data and graphical interface from NOAA ESRL, 2009b.) (d) NAO index (Hurrell, 1995, 2009): difference of sea level pressure between Lisbon, Portugal and Stykkisholmur, Iceland. *Source: Updated by Hurrell (personal communication, 2011).* (e) EAP index: amplitude of second EOF. *Source: From NOAA ESRL (2009b).* (f) AMO: amplitude of the principal component of proxy temperature records. *Source: From Delworth and Mann (2000).* (g) Time series, each with a 10-year running mean and "normalized" by its maximum amplitude. NAO and EAP as above. The AMO is the Enfield et al. (2001) SST-based index.

top to bottom. Labrador Sea Water (LSW), Greenland Sea Deep Water, and Eighteen Degree Water (EDW) all vary with the NAO (Dickson et al., 1996). During positive NAO, when the subpolar gyre and Labrador Sea are cold, LSW production is strong and anomalously cool. The Greenland Sea, on the other hand, is warmer during high NAO, and Greenland Sea Deep Water production is weakened and warmer (Section S15.5.3). EDW production is also weaker during periods of high NAO, nearly ceasing in the mid-1970s and shifting to lower densities in the 1990s (Dickson et al., 1996; Talley, 1996b).

Decadal variability in the northern North Atlantic is also associated with the *East Atlantic Pattern* (EAP) (Barnston & Livezey, 1986; Josey & Marsh, 2005; Figure S15.2b and e). Decades long freshening of the subpolar gyre (described in the following section) appears to be related to increased precipitation associated with increasing EAP. The EAP and NAO are independent. The EAP is the second empirical orthogonal function (EOF) of climate variability for the Atlantic, while the NAO can be defined as the first EOF. The EAP has a zero crossing around 35°N that is farther south than that of the NAO, and a symmetric shape about the equator. It appears to be the lowest order symmetric (sinelike) meridional mode for the Atlantic.

The Atlantic's longer term variability is of interest because of its potential relationship to variability in the MOC. The *Atlantic Multidecadal Oscillation* (AMO) or "Atlantic Multidecadal Variability" is an index of Atlantic SST used to quantify variability at timescales longer than decadal. The AMO index is the average SST anomaly for the entire North Atlantic (0–70°N), detrended, and with a 10-year running mean applied (Enfield, Mestas-Nuñez, & Trimble, 2001). When the index is positive, the North Atlantic as a whole is warm and the South Atlantic is cool; this is thus an "interhemispheric mode" (Figure S15.2c). Monthly values of the index since 1856 are available through the NOAA ESRL (2009b) Web site, listed as an updated "Kaplan SST" product (Kaplan et al., 1998). The AMO timescale is 65–80 years with a range of several 0.1 °C. There are only two "cycles" in the SST record. However, longer paleoclimate proxy records also show an AMO (Delworth & Mann, 2000; Figure S15.2f). The AMO can also be reproduced with coupled ocean-atmosphere models that include meridional overturning circulation changes.

An interhemispheric mode described as the "bipolar seesaw" has been introduced to explain much longer timescale (millennial) variability in paleoclimate records at the end of the last glaciation during the Younger Dryas interval (Broecker, 1998). These records include signals in the far Northern and far Southern Hemispheres that are out of phase with each other. These could be explained by a climate mode with north-south structure like that of the AMO. With a strong MOC, there would be enhanced northward transport of heat into the subpolar gyre and Nordic Seas, and SST would then be higher there. There would also be enhanced northward cross-equatorial flow of warm water removing heat from the South Atlantic and moving it to the North Atlantic.

The NAO also has a multidecadal timescale (Delworth & Mann, 2000; Visbeck, 2002), as shown using a 10-year running mean of its index (Figure S15.2g). The EAP also has decadal variability (also seen in Figure S15.2g), which has some resemblance to the AMO index after about 1970. The EAP has been associated with the decadal Great Salinity Anomalies described in the next section.

S15.2.3. Atlantic Ocean Property Variability

Changes in the Atlantic's MOC, whether natural or anthropogenic, both reflect and have the potential for affecting Earth's climate

(Vellinga & Wood, 2002). Since the late 1990s, there have been coordinated programs to monitor the Nordic Seas overflows, the Labrador Sea, the Strait of Gibraltar, and meridional overturn at several latitudes in the North Atlantic with most resources across 24°N. Broad-scale observations are providing the larger context for the changes. SST is monitored widely; its variations relative to the various Atlantic climate modes were shown in Figures S15.1 and S15.2.

We focus here on variability in surface salinity as it provides a control on mixed layer depth and density. Over the past century, subpolar North Atlantic SSS variations have been significant (Figure S15.3a). After a fresh period centered around 1910, salinity was relatively high at 60°N until the 1970s. Salinity then declined and remained low until about 2000, with the continuing freshening a subject of great interest because of its potential for slowing the North Atlantic MOC (Curry, Dickson, & Yashayaev, 2003; Dickson, Curry, & Yashayaev, 2003). After 2000, the salinity trend reversed, with salinity now increasing throughout the subpolar gyre. This has joined the upward salinity trend over the past 50 years in the remainder of the Atlantic (Figure S15.20 in Section S15.7).

Looking at decadal timescales within the longer term salinity record, there are clear pulses of fresher water in the mid-1970s, 1980s, and 1990s. Along with the 1910 event, these have been called *Great Salinity Anomalies* (GSAs; Dickson, Meincke, Malmberg, & Lee, 1988; Belkin, 2004). The low salinity GSAs form coherent, time-lagged patterns around the northern North Atlantic and Nordic Seas. The 1970s GSA emerged from Fram Strait into the East Greenland Current in 1968 (Dickson et al., 1988; Figure S15.3b). The pulse of freshwater appeared to move down around Greenland, into the Labrador Sea, out into the North Atlantic Current, and into the eastern subpolar gyre, returning to the Nordic Seas about 10 years later. Low salinity anomalies with similar propagation patterns occurred in the 1980s and the 1990s, with both events originating from the Canadian archipelago into the Labrador Sea. The GSAs in the northern Labrador Sea are closely related to sea ice extent in Davis Strait, which is the northern entrance to the Labrador Sea from the Arctic (Deser, Holland, Reverdin, & Timlin, 2002).

Because it is unlikely that anomalies of the magnitude of GSAs could advect all the way around the cyclonic circulation for up to 10 years with little change in amplitude, it has been hypothesized that GSAs arise at least partially in response to adjustment of the circulation and its fronts (Sundby & Drinkwater, 2007). Whatever the mechanism, when upper ocean low salinity anomalies arrive, SST patterns are altered, convection is inhibited, and there may be feedbacks into the climate modes (Zhang & Vallis, 2006).

Large-scale salinity changes have been observed at depth in the northern North Atlantic (e.g., in the Labrador Sea Water in Figure S15.4). In the 1960s, during a period of low NAO, the Labrador Sea was warm and saline at all depths; LSW formation was weak and relatively warm and saline. By the 1990s, LSW properties had shifted to fresher, colder, and denser (high NAO). Freshening occurred throughout the northern North Atlantic at intermediate depths (Dickson et al., 2002). In the later 1990s, LSW production again was interrupted, and its temperature and salinity began to increase (declining NAO; Yashayaev, 2007; Schott, Stramma, Giese, Zantopp, 2009). Although salinity had shifted to a fresher range in the1990s, the spatial structure of salinity did not change: lowest salinity in the Labrador Sea with tongues of low salinity extending to the Irminger Sea, Iceland Basin, and Rockall Trough and a weak tongue extending southward around Newfoundland. Thus the overall circulation pattern was mostly preserved.

The freshening of deep waters throughout the northern North Atlantic and the southern

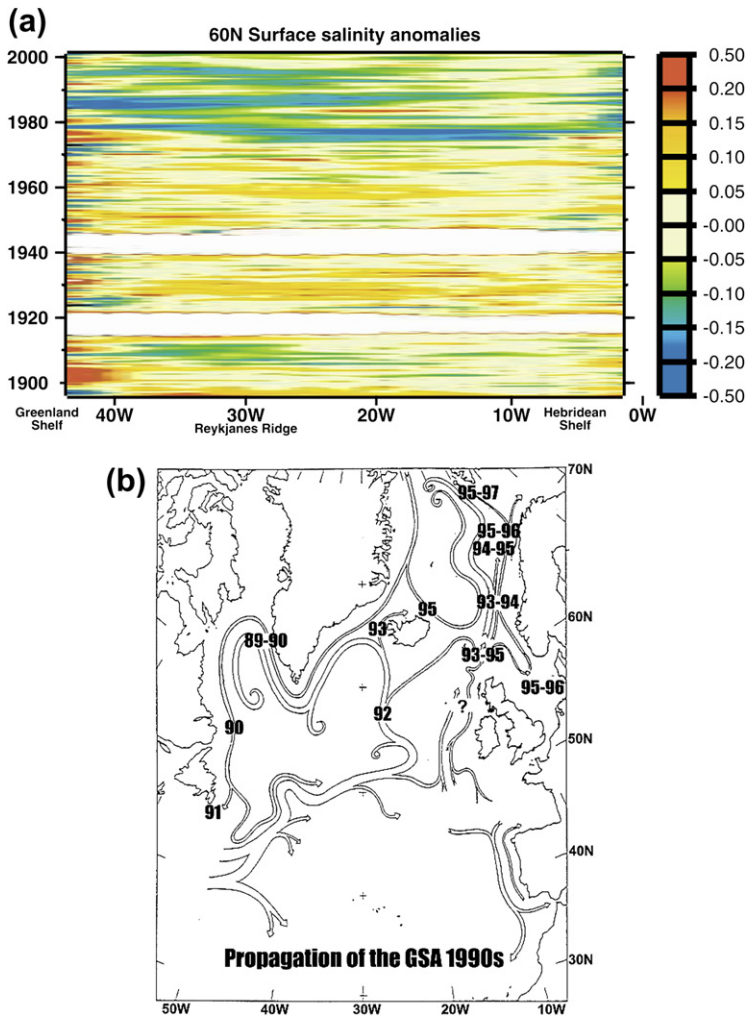

FIGURE S15.3 North Atlantic surface salinity variability. (a) Salinity anomalies relative to long-term mean along 60°N. *Source: From Reverdin et al. (2002).* (b) Great Salinity Anomaly: timing in years for the 1990s GSA. *Source: From Belkin (2004).*

Nordic Seas through the 1990s was accompanied by freshening of the Nordic Seas overflows as well (Dickson et al., 2002, 2003). These overflow property variations result from (1) changes upstream in the Nordic Seas and (2) the previously mentioned changes in the entrained upper ocean and intermediate waters as the overflows plunge toward the ocean bottom. On the other hand, the overflows have been remarkably steady in terms of velocities, transport, and temperature, mainly because of the importance of hydraulic control at the straits, governed by the large upstream reservoir in the Nordic Seas (Girton, Pratt, Sutherland, & Price, 2006). In Faroe Bank Channel, transports, bottom velocities, and bottom temperature held steady at 2.1 Sv, >100 cm/sec, and -0.4 °C for the directly observed period from 1995 to 2005 with indirect evidence for similar stability based on observations starting in 1948 (Olsen, Hansen, Quadfasel, & Østerhus, 2008). In Denmark Strait, four years of monitoring showed more

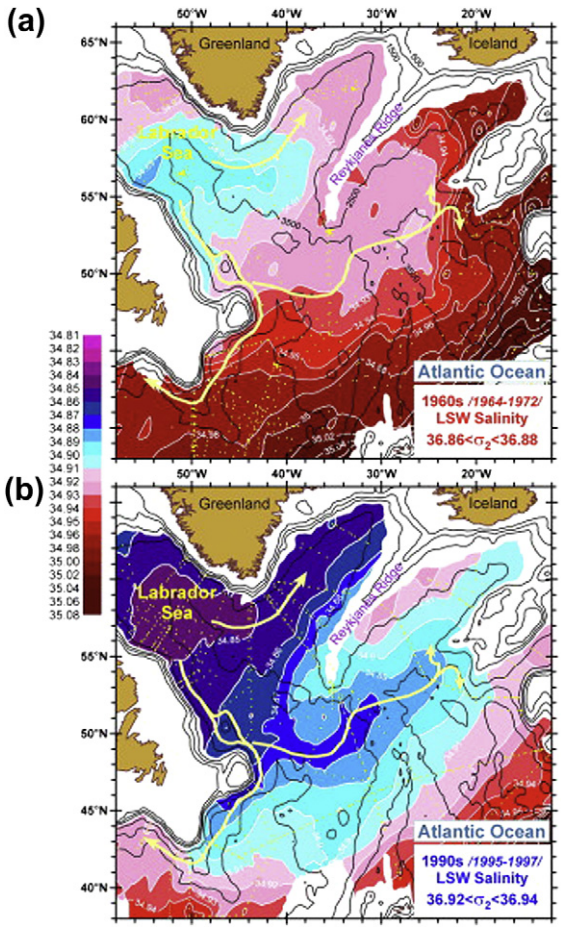

FIGURE S15.4 Salinity at the density of LSW in two different decades: (a) 1960s and (b) 1990s. *Source: From Yashayaev (2007).*

variability in overflow velocities, transports, and temperatures than at Faroe Bank (Macrander et al., 2005). Transports ranged from 3.1 to 3.7 Sv and temperatures varied by 0.5 °C. Higher transports corresponded roughly with colder water. Hydraulic control is important, as in Faroe Bank Channel, but there are other dynamical processes, such as wind-driven northward flow in the eastern Denmark Strait, that can modulate the overflow transport.

The variable properties in the intermediate and deep waters of the northern North Atlantic move southward into the subtropics and tropics, mainly through the Deep Western Boundary Current. Changes in properties including oxygen have been documented at the Grand Banks (~43°N), at Abaco (26.5°N), and all the way to the equator with appropriate time lags of 2 to 10 years from changes at the subpolar sources (Molinari et al., 1998; Stramma et al., 2004; Bryden, Longworth, & Cunningham, 2005b). On the other hand, DWBC transport variations that can be associated with changes in the MOC have been difficult to document from sparse decadal hydrographic sampling because large seasonal variability is aliased to longer timescales. However, with the now continuous monitoring at ~25°N, including the Florida Current and basin-wide Ekman transport as well as the DWBC, the prognosis for monitoring interannual variations in the total overturn is good to within about 10% of the total overturn (Cunningham et al., 2007).

S15.2.4. Climate Change and the Atlantic Ocean

As introduced in Section S15.1, climate change is the response of the climate system to anthropogenic forcing, as distinguished from natural climate variability. There is great interest in determining if the Atlantic's MOC is changing in response to anthropogenic forcing, because this would presumably change the amount of ocean heat transport to high northern latitudes. However, because of the large amplitude of natural variability in the northern North Atlantic, mostly associated with the NAO and possibly also the EAP, and because of the short length of observational records, attribution of circulation and local water mass variations to anthropogenic forcing has not yet been possible (Bindoff et al., 2007). Detection of long-term trends indicative of climate change has only been possible for properties averaged over very large areas.

Heat content in the Atlantic Ocean has increased overall during the last several decades

(Figures S15.18 and S15.19 in Section S15.7). The upper ocean warmed except between 50 and 60°N where cooling was due to a positive trend in the NAO index, which peaked in the early 1990s; positive NAO is associated with cooling in the Labrador and Irminger Seas (Figure S15.2a). In the North Atlantic, the deep penetration of warming in the subtropics was due to warming Mediterranean Water and reduced production of LSW. The world ocean as a whole warmed during those five decades; the Atlantic contributed the most to the overall trend (Levitus, Antonov, & Boyer, 2005). Attribution of the warming in the North and South Atlantic to anthropogenic change has been made by use of coupled climate model simulations run with and without anthropogenic forcing (Barnett et al., 2005; see Chapter 14).

Salinity trends in the Atlantic during the same five decades included regions that increased and decreased in salinity (Figure S15.20 in Section S15.7). Freshening in the northern North Atlantic between 45 and 75°N (Section S15.2.3) began in the mid-1970s. This has reversed to increasing salinity since the year 2000. Overall, the Atlantic salinity has increased (while the Indian has increased and the Pacific salinity has decreased for a global balance of no net change). Attribution of the observed salinity changes to anthropogenic forcing is more indirect than for temperature change. However, the changes in salinity are consistent with anthropogenic change since a warmer atmosphere can hold more moisture (Section S15.7).

S15.3. CLIMATE AND THE PACIFIC OCEAN

The Pacific Ocean represents a large fraction of the global ocean's surface and therefore a large potential for coupled atmosphere-ocean feedbacks. The interannual ENSO (Section 10.8), which has maximum amplitude in the tropics, is an excellent example of efficient coupling. The decadal and longer timescale climate modes are characterized by much larger north-south spatial patterns with extratropical amplitudes that are similar to tropical amplitudes. Outside the tropics, coupling of the ocean and atmosphere is much weaker, so feedbacks are much weaker and harder to discern.

Good resources for the many climate modes are found on the National Oceanic and Atmospheric Administration's (NOAA) various climate Web sites, including the Climate Diagnostics Center (Climate Analysis Branch; http://www.cdc.noaa.gov/) and the National Weather Service's Climate Prediction Center (http://www.cpc.ncep.noaa.gov/).

Pacific "decadal" climate variability has a timescale of 15 to 20 years, which is longer than the dominant Atlantic decadal timescales. The difference in timescale may reflect the size of the ocean basins and hence timescale for planetary wave propagation. Decadal Pacific modes include the *Pacific Decadal Oscillation* (PDO) and the *North Pacific Gyre Oscillation* (NPGO; Mantua et al., 1997; Di Lorenzo et al., 2008). These are the first and second EOFs of SST in the North Pacific (Figures 6.11 and 6.12 from Davis, 1976; Cayan, 1992). Two related North Pacific indices based on atmospheric pressure are the *Pacific North American* teleconnection pattern (PNA) and the *North Pacific Index* (NPI; Trenberth & Hurrell, 1994). The *Southern Annular Mode* (SAM) is a circumpolar mode with major impacts on the South Pacific (Thompson & Wallace, 2000).

The PDO spans the whole Pacific, although it is most robust in the North Pacific (Figure S15.5a). Its pattern is nearly symmetric about the equator, with high amplitude centered broadly on the equator and out-of-phase amplitude centered in the subtropical/subpolar North and South Pacific. The strength of the Aleutian Low is associated with the PDO. When the Aleutian Low is strong (high PDO), the westerly winds are strong and displaced

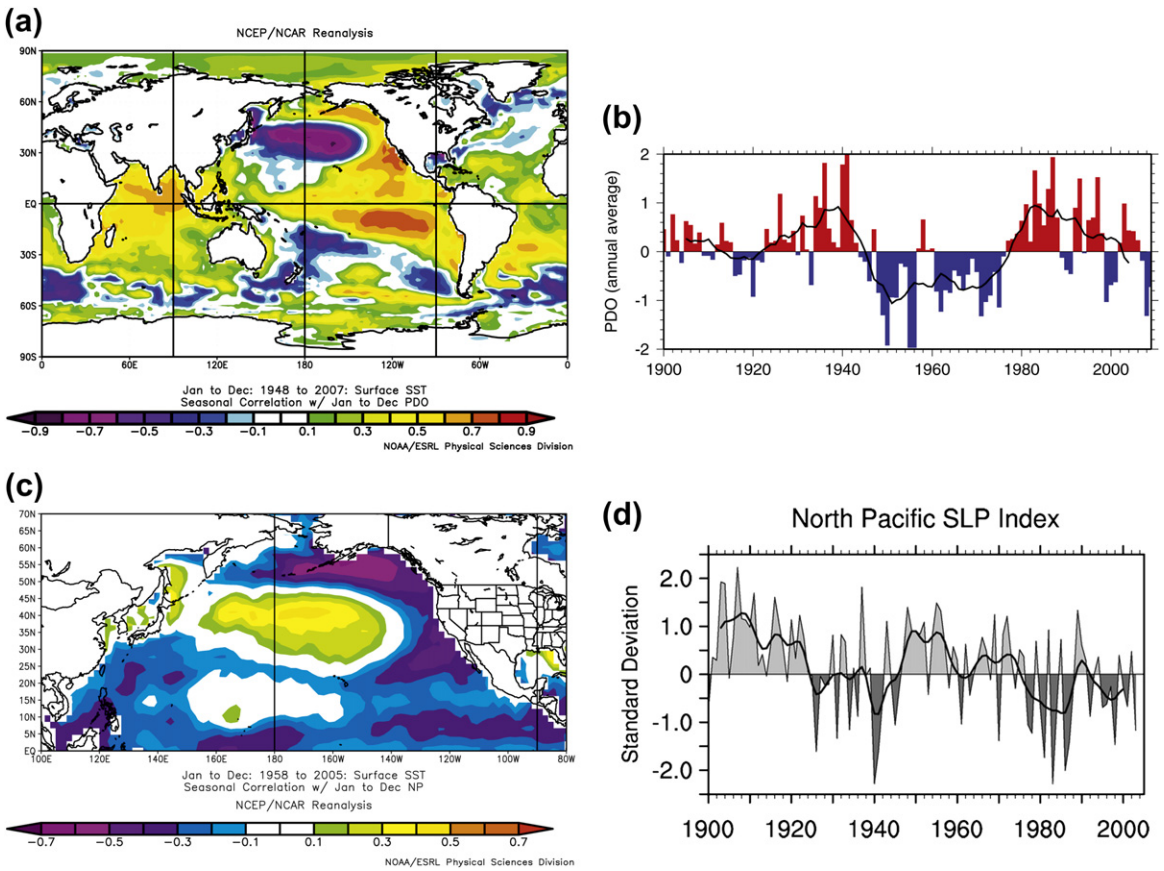

FIGURE S15.5 Pacific Decadal Oscillation (PDO) and North Pacific Index (NPI). (a) SST correlation with the PDO index. (b) Annual mean PDO index (red/blue) and with a 10-year running mean (black). (Updated from Mantua et al., 1997 and Trenberth et al., 2007). (c) NPI SST pattern. (Data and graphical interface for a, b, and c from NOAA ESRL, 2009b). (d) NPI index. ©American Meteorological Society. Reprinted with permission. *Source: From Deser, Phillips, & Hurrell (2004).*

somewhat to the south; the ocean's subpolar gyre is strong and less subpolar water enters the California Current system. This means that the entire eastern boundary region, for both the subpolar and subtropical gyres, is warmer than normal, while the central Pacific, beneath the strengthened westerlies, is abnormally cold. The Oyashio is strong and penetrates farther southward along the coast of Japan.

A well-documented shift from low to high PDO occurred around 1976. At this point, a lengthy period of a particularly strong Aleutian Low began. The changes in ocean temperatures and circulation resulted in marked shifts in almost every environmental variable measured in the North Pacific — fish, birds, crabs, salinity, nutrients, and so forth (Mantua et al., 1997).

The NPGO has a tighter spatial pattern than the PDO since it is a higher mode EOF (Figure S15.6). The NPGO is much better correlated than the PDO with environmental variables such as upwelling and ecosystem production along some large portions of the North Pacific coastline.

The NPI is the mean sea level pressure over the region 30–65°N, 160°W–140°W and as

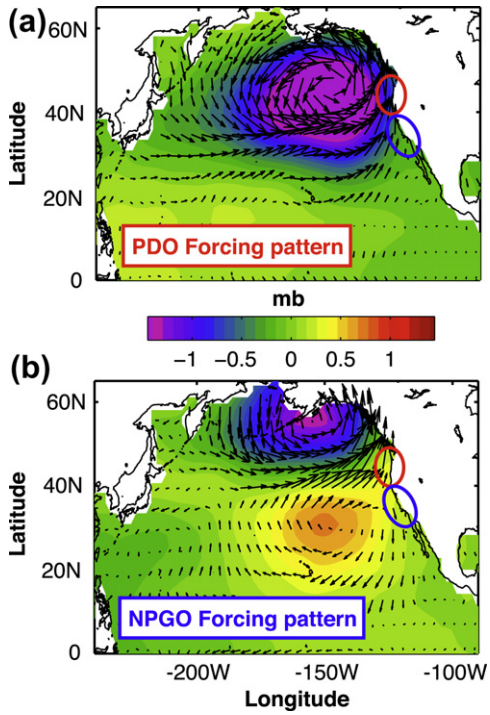

FIGURE S15.6 (a) Pacific Decadal Oscillation (PDO) and (b) North Pacific Gyre Oscillation (NPGO) patterns of sea level pressure (color) and surface wind stress (vectors). The PDO/NPGO are correlated well with upwelling in the red-circled/blue-circled region off Oregon/California. *Source: From Di Lorenzo et al. (2008).*

such is a direct measure of the strength of the Aleutian Low (Trenberth & Hurrell, 1994). The PNA is an older index of atmospheric geopotential height, summed from four locations, including two over North America. Their SST patterns are virtually identical. The NPI and PDO patterns and time series are very similar (Figure S15.5). The PDO could be considered a combination of ENSO and the NPI, that is, a combination of tropical forcing and Aleutian Low forcing (Schneider & Cornuelle, 2005).

The Southern Annular Mode (SAM), also known as the Antarctic Oscillation (AAO), dominates decadal variability at high southern latitudes (Section S15.6). One of the centers of maximum amplitude of the SAM pattern is in the western South Pacific, centered at New Zealand (Figure S15.15 in Section S15.6). Variability in circulation in the South Pacific subtropical gyre has been linked to the SAM (Roemmich et al., 2007).

Climate change in response to anthropogenic forcing has been documented in the Pacific as well as in the other main oceans (Section S15.7). The upper 500 m of the Pacific has warmed over the past 50 years (Figure S15.19) as part of the general warming of the global ocean (Levitus et al., 2005). Basin-averaged salinity has decreased slightly but measurably (Boyer, Antonov, Levitus, & Locarnini, 2005). Fresh intermediate water masses such as *North Pacific Intermediate Water* (NPIW) and *Antarctic Intermediate Water* (AAIW) (Section 10.9.2) have freshened (Wong, Bindoff, & Church, 2001).

Oxygen content has been decreasing in most parts of the upper Pacific Ocean over the past 50 years. The tropical oxygen minimum zones have expanded (Stramma, Johnson, Sprintall, & Mohrholz, 2008) and oxygen has declined throughout the upper ocean in the North Pacific and in the Antarctic Circumpolar Current (ACC) region (Deutsch, Emerson, & Thompson, 2005; Aoki, Bindoff, & Church, 2005). The Pacific Ocean has become more acidic; it appears that there is no possibility of reversing the trend given the relentless increase in atmospheric CO_2 content. Stresses on ecosystems such as coral reefs and continental shelves resulting from increased temperatures and acidity are beginning to be observed.

S15.4. CLIMATE AND THE INDIAN OCEAN

Climate variability at interannual to decadal timescales has been documented in the Indian Ocean. Because of its importance to agriculture, interannual and longer term variability in the monsoon has been of special interest. In fact,

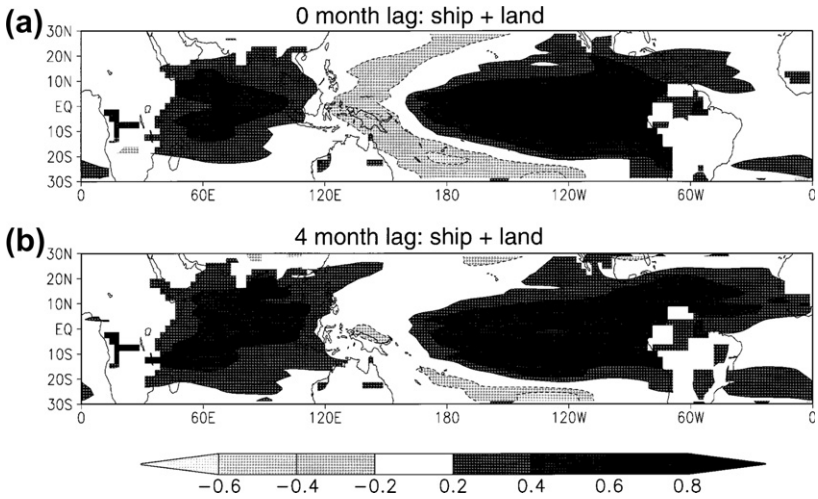

FIGURE S15.7 Correlation of SST anomalies with the ENSO index for 1982–1992, at (a) 0 month lag and (b) 4 month lag. ©American Meteorological Society. Reprinted with permission. *Source: From Klein, Soden, and Lau (1999).*

while working in the early twentieth century on understanding the sources of monsoon variability (including an especially devastating monsoon failure in 1899), Sir Gilbert Walker detected and documented the Southern Oscillation, which is the interannual variability in the zonal atmospheric pressure gradient between the central tropical Pacific and the western Pacific/eastern Indian Ocean (Section 10.8). His was the first major step toward documenting and understanding the interannual ENSO of the Pacific Ocean.

Although the air–sea coupling process that creates ENSO is centered in the tropical Pacific, ENSO dominates interannual climate variability in the Indian Ocean (Tourre & White, 1995, 1997). During an El Niño event in the Pacific, SSTs in the tropical Indian Ocean rise 3–6 months later (Figure S15.7). El Niño also affects precipitation in the Indian Ocean region, including dry conditions in India in the Northern Hemisphere summer and in eastern Africa in austral summer (see global ENSO precipitation anomaly maps in online supplementary Figure S10.43).

At the onset of an El Niño event in the Pacific, anomalously easterly winds in the Indian Ocean cause upwelling in its eastern region and depress the thermocline in the western region, initially resulting in cooling in the east and warming in the west as observed. As El Niño progresses, changes in surface heat flux cause the entire tropical Indian Ocean to warm (Klein, Soden, & Lau, 1999). Feedbacks between the ocean and atmosphere within the Indian Ocean then affect the local response to El Niño (Zhong, Hendon, & Alves, 2005). The development of the Indian Ocean response to El Niño depends on the phase of a given El Niño event relative to the monsoon, because the seasonal monsoon affects SST in the western tropical Indian Ocean, which then affects the local air–sea feedbacks (Krishnamurthy & Kirtman, 2003). The Indian Ocean is "upstream" of the Pacific Ocean in terms of an atmospheric signal called the Madden-Julian Oscillation (MJO). The MJO has a period of 30 to 60 days and affects all atmospheric variables including winds, clouds, rainfall, and air–sea fluxes (Madden & Julian, 1994; NOAA CPC, 2005). MJO events begin in the Indian Ocean and propagate eastward. They often provide the westerly wind bursts that affect the onset of El Niño in the western Pacific (Section 10.8).

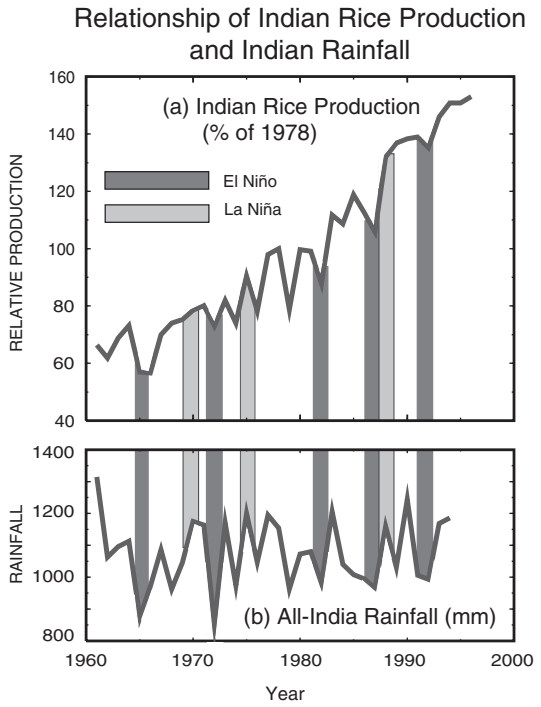

FIGURE S15.8 Indian Ocean. Changes in (a) rice production and (b) rainfall in India with El Niño and La Niña events indicated. The long-term trend in production is due to improved agricultural practices. (Adapted by WCRP, 1998 from Webster et al., 1998.)

The Indian monsoon is affected by ENSO. The Southwest Monsoon is weak during El Niño events, leading to the "dry" years with reduced agricultural production in India (Figure S15.8; Webster et al., 1998).

Beyond its response to ENSO, the Indian Ocean has internal interannual variability. A tropical IOD mode has been described whose positive phase is characterized by warm SST anomalies in the western tropical Indian Ocean and cool anomalies in the eastern tropical region (Figure S15.9a). These SST anomalies are accompanied by zonal wind anomalies that blow from the cool region to the warm and higher amounts of rainfall over the warm region. The simplest index is the east-west difference in tropical SST (Figure S15.9b; Saji, Goswami, Vinayachandran, & Yamagata, 1999; Webster, Moore, Loschnigg, & Leben, 1999). Studies of the complete Indian-Pacific region suggest that the mode might not be entirely independent of ENSO, and that this internal Indian Ocean mode can be excited by ENSO (Krishnamurthy & Kirtman, 2003; Zhong et al., 2005). High correlation between ENSO and the dipole mode occurred from 1960 to 1983 and after 1993, but not in the intervening period (Clark, Webster, & Cole, 2003). It is also possible that the relationship between ENSO and the dipole mode has changed over time and that the dipole mode could be excited by other climate variability (Annamalai, Xie, McCreary, & Murtugudde, 2005; Ihara, Kushnir, & Cane, 2008).

Ocean circulation in the northern Indian Ocean, including the Arabian Sea and Bay of Bengal, is dominated by the seasonal monsoon wind forcing and so it should respond to interannual variability in the monsoon strength. The monsoon response is especially strong in the upper 200 m, with almost no effect in the abyss, so that strong response might be expected in the upper ocean (Dengler, Quadfasel, Schott, & Fischer, 2002). However, interannual variability observed in Arabian Sea circulation is more complicated than a simple direct response to changing monsoons. Planetary (Rossby) wave propagation across the Arabian Sea is important for adjustment of the circulation to changes in winds and affects the time phasing of the circulation response (Schott & McCreary, 2001).

Comprehensive, long-term in situ observations that could be used to describe decadal and longer term climate variability within the Indian Ocean's water column are sparse and descriptions are therefore lacking. Relative to climate change, trends and changes observed in Indian Ocean water properties and circulation were summarized in the IPCC Fourth Assessment Report (Bindoff et al., 2007). The Indian Ocean's upper layer warmed over the past 50 years except at the base of the mixed layer at the equator and southward through

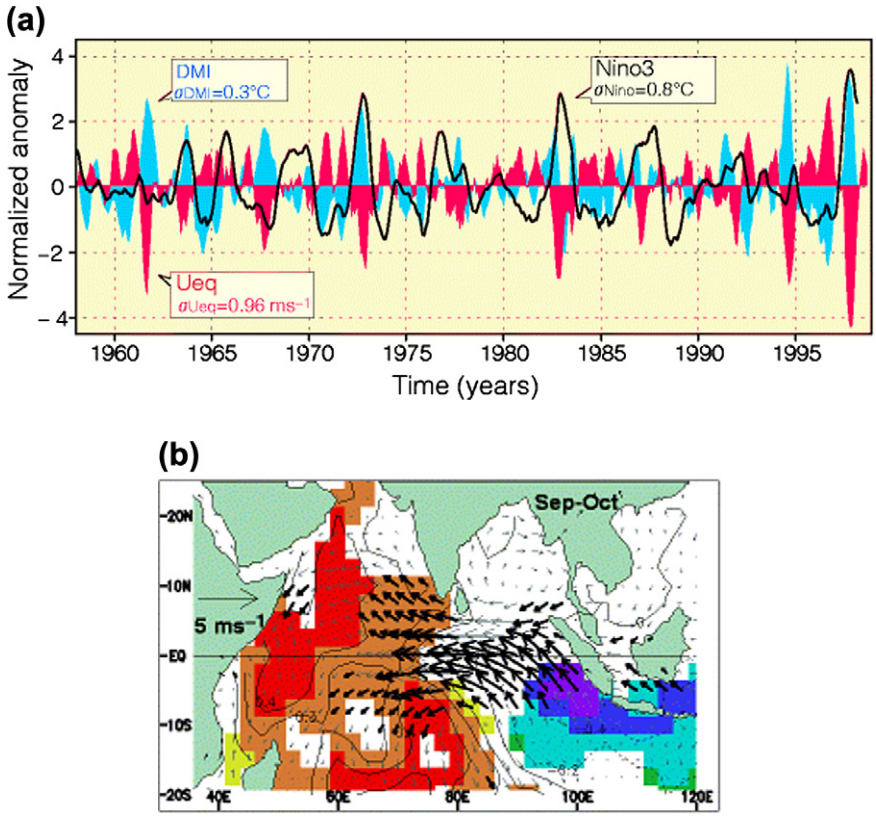

FIGURE S15.9 Indian Ocean Dipole mode. (a) Anomalies of SST (shading) and wind velocity (arrows) during a composite positive IOD event. These are accompanied by higher precipitation in the warm SST region and lower precipitation in the cool SST region. (b) IOD index (blue: difference in SST anomaly between the western and eastern tropical Indian Ocean), plotted with the anomaly of zonal equatorial wind (red) and the Nino3 index from the Pacific (black line). *Source: From Saji et al., (1999).*

the SEC, similar to the warming pattern in the Pacific (Figures S15.18 and S15.19 in Section S15.7; Levitus et al., 2005). Salinity in the upper ocean also increased overall, similar to salinity increase in the Atlantic but opposite the slight freshening of the Pacific (Boyer et al., 2005).

Circulation in the south Indian Ocean's subtropical gyre likely increased by about 20% between the late 1980s and early 2000s based on tracers indicating ventilation (McDonagh et al., 2005). There was a slowdown of similar strength between the 1960s and 1980s (Bindoff & McDougall, 2000). The increased circulation through the 1990s was associated with strengthening westerlies, as measured by the SAM index (Section S15.6). It is not yet clear whether these shifts in circulation and forcing are due to climate change or are a natural climate fluctuation.

S15.5. CLIMATE AND THE ARCTIC OCEAN

S15.5.1. Arctic Oscillation, Atlantic Multidecadal Oscillation, and Global Change

Three modes of climate variability/change are frequently used for describing Arctic

variability: the *Arctic Oscillation* (AO; also called the *Northern Annular Mode*), the *Atlantic Multidecadal Oscillation* (AMO), and global change driven by anthropogenic forcing. The AO and AMO are natural modes. The AO has decadal to centennial variability, and is closely related to the North Atlantic Oscillation (Section S15.2). AO variability affects the winds, so variations in the ocean circulation and ice drift in the Arctic and northern North Atlantic are closely tied to the AO. The AO does not appear to be a coupled ocean-ice-atmosphere climate mode, but rather a mode of the atmosphere. The AMO might be a natural mode of multidecadal variability of the Atlantic MOC (Section S15.2). Global change effects are detected as long-term trends with attribution based on the distinctive signature of changes in winds, atmospheric pressure, temperature, and so forth.

The AO is a variation in the atmospheric pressure and wind pattern in middle and high northern latitudes (Thompson & Wallace, 1998). The prevailing wind pattern over the Arctic is the westerly "polar vortex" with low atmospheric pressure at the pole and higher pressure at mid-latitudes (see schematic in NSIDC, 2009b). This can be described in terms of the dominant EOF of the sea level pressure pattern north of 20°N, using only winter months (JFMA) for the EOF (Thompson & Wallace, 1998). The AO index (Figure S15.10c) is the amplitude of this dominant EOF.

When the AO is in its positive phase (illustrated by the correlation pattern in Figure S15.10b), polar pressure is lower than usual, the difference in pressure between the highs at mid-latitudes and the polar low is larger, and the polar vortex is stronger and is shifted toward the north. There is wetter, warmer weather in the subpolar regions (and drier conditions in mid-latitudes) since the mid-latitude high pressure extends farther north, and the storm track is shifted farther north. Temperatures over Labrador, Greenland, and the western subpolar North Atlantic drop. When the AO is in its negative phase, the difference in pressure is reduced, the polar low-pressure region is larger, the polar vortex is weaker, and the storm tracks shift to the south; this results in colder, drier weather at the higher latitudes.

During positive AO, the Transpolar Drift (TPD) flows nearly directly across the Arctic from Bering Strait to the northern side of Greenland and the Beaufort Gyre is restricted to the side of the Canadian Basin. During negative AO, the Beaufort Gyre expands and strengthens and the TPD shifts toward the Lomonosov Ridge (Rigor, Wallace, & Colony, 2002; Figure 12.14a from Steele et al., 2004).

Over the past century, the AO was relatively high into the 1930s, then alternated or shifted to low in the 1960s and 1970s. Since a sudden peak in 1989, it has been generally high, with much interannual and decadal variability about these longer term signals (Figure S15.10c).

The AMO is a natural climate mode of the Atlantic Ocean (Section S15.2.2) and also affects the Nordic Seas and Arctic. It is entirely independent of the AO and NAO. During periods of high AMO, northern North Atlantic SSTs are high and the MOC is strong, advecting warm waters farther northward. During low AMO, the overturning circulation is weak and the northern North Atlantic and Nordic Seas cool off. The AMO index time series (Figure S15.2) is remarkably similar to multidecadal fluctuations in the Atlantic Water temperature within the Arctic Ocean (Figure S15.13), suggesting a link between the meridional overturning strength and upper ocean temperatures far into the Nordic Seas/Arctic (Polyakov et al., 2005).

Long-term variability in the Arctic and Nordic Seas can involve climate system feedbacks. The simplest and possibly most important is the "ice-albedo feedback" (Figure 5.10). Changes in sea ice also affect atmospheric winds, which sense the large temperature difference between the ice and open water. A feedback involving sea ice and wind in the Beaufort Gyre is centered on the difference in

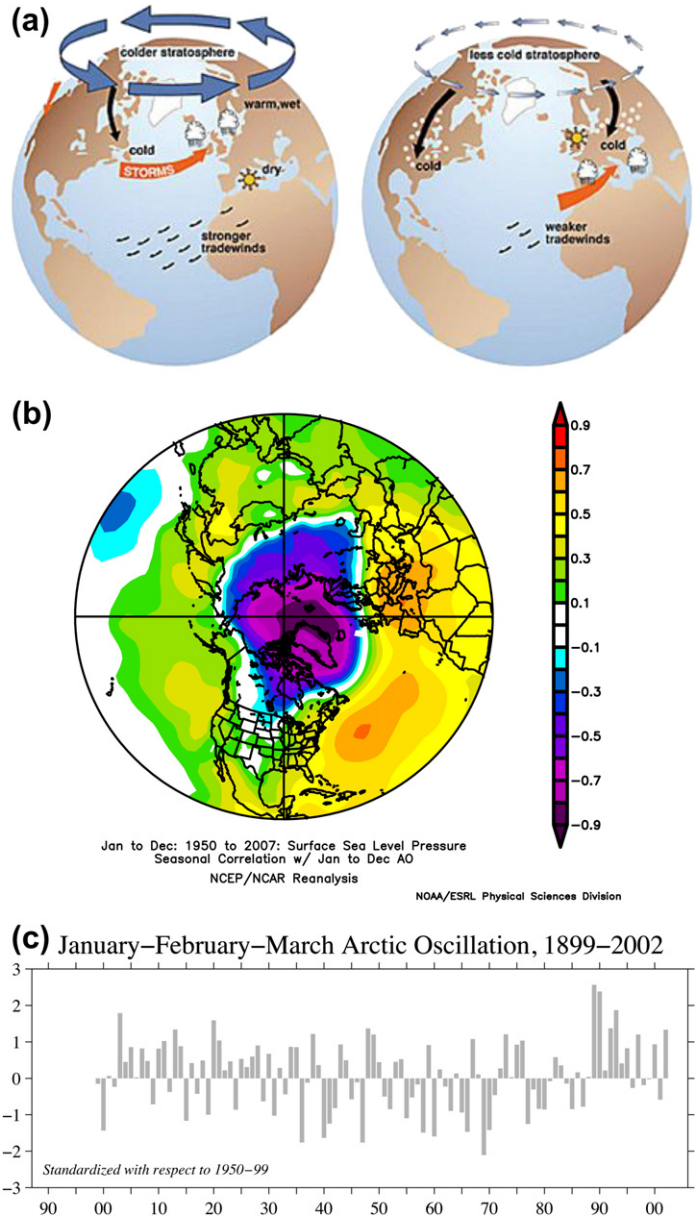

FIGURE S15.10 Arctic Oscillation (AO). (a) Schematics of (left) the positive phase and (right) the negative phase (NSIDC, 2009b). (b) Correlation of surface pressure (20 −90°N) with the AO index for 1958 to 2007. (Data and graphical interface from NOAA ESRL, 2009b.) (c) Arctic Oscillation index 1899−2002. *Source: From JISAO (2004).*

surface currents when driven directly by wind or by wind acting on the ice (Shimada et al., 2006).

Global change resulting from anthropogenic forcing, mainly greenhouse warming, has a strong signature in the Arctic, which has warmed nearly twice as much as the global average over the past 100 years (IPCC, 2007). Greatest surface warming as a result of global change is predicted for the highest northern

latitudes; this is referred to as "polar amplification," although it is a feature of just the Arctic and not the Antarctic. Greater warming occurs at the Arctic's surface than at lower latitudes for a number of reasons: the ice-albedo feedback, the increased amount of water vapor in the atmosphere that changes the polar radiation balance in the atmosphere, and the thinness of the polar troposphere over which the heat is distributed.

S15.5.2. Variations in Arctic Sea Ice

Arctic sea ice extent and volume have been decreasing and the ice has become younger and thinner since the late 1970s (Rothrock, Yu, & Maykut, 1999; Fowler, Emery, & Maslanik, 2004). Multi-year ice has been declining in areal extent (Figures 12.22 and S15.11), even taking into account considerable interannual variation. Each year has brought continued decrease in ice cover and additional diagnoses of the causes (Serreze, Holland, & Stroeve, 2007). Causes of the sea ice reduction have been linked to both the positive phase of the naturally occurring AMO and to global warming. Indeed, global warming might contribute to a positive AO, and could likely impact the AMO (IPCC, 2007).

From the beginning of the satellite observations of ice cover in 1978 to the present, Arctic ice cover has decreased relentlessly, although the record includes the usual short-term fluctuations/noise of climate records (Figure S15.11).[2] (This highlights the importance of observing continuously for many years before it is possible to discern a trend.) Ice cover in 2007 relative to the mean extent for previous decades illustrates the dramatic trend in ice cover (Figure S15.11). Once the ice decline had progressed long enough to be noticed even in the noisy climate record, it became apparent that much of the ice loss is in the perennial ice pack (multi-year ice), which means that thinner, seasonal ice has increased in relative importance (Johannessen, Shalina, & Miles, 1999). Largest changes have taken place in the Beaufort and Chukchi Seas, with more than 25% reduction (Maslanik, Serreze, & Agnew, 1999; Shimada et al., 2006). Since first-year, thin ice melts away more readily in summer, reducing the overall albedo of the Arctic, the stage continues to be set for further decline of ice cover through ice-albedo feedback (Figure 5.10). (Note though that there are multiple reasons for the decline in addition to this feedback.)

Large interannual variations in ice cover that persist for 5–7 years are associated with changes in the wind-forced circulation (Proshutinsky &Johnson, 1997), possibly associated with variations in the AO. In the mid-1990s, during positive AO (Figure S15.10c), the cold halocline weakened, which increased ocean heat flux and a decrease in sea ice (Martinson & Steele, 2001). The AO returned closer to neutral in the mid-1990s, but sea ice continued to decrease, with an even greater loss in 2007, repeated in 2008, than expected from the trend (Figure S15.11c). The Pacific sector north of Bering Strait has shown the greatest decline (Figure S15.11a,b and Shimada et al., 2006). The AMO shifted to a high phase in the late 1990s and the incursion of warm Atlantic Water into the Arctic continued, separate from the AO variability; this likely has contributed to the decreasing sea ice.

There are many ways to reduce sea ice during the positive phase of the AO. Changes in Arctic winds (direction) can result in warmer air that melts ice. Changes in circulation during a positive AO include greater penetration of warm Atlantic Water into the Arctic, which also melts ice. Changing winds in positive AO increase movement of sea ice away from the coasts of the Eurasian Basin, resulting in younger, thinner

[2] The maps and time series in Figure S15.11 show September ice cover changes because September is at the end of summer. The September sea ice record represents the amount of ice that can remain as multi-year ice during the succeeding year.

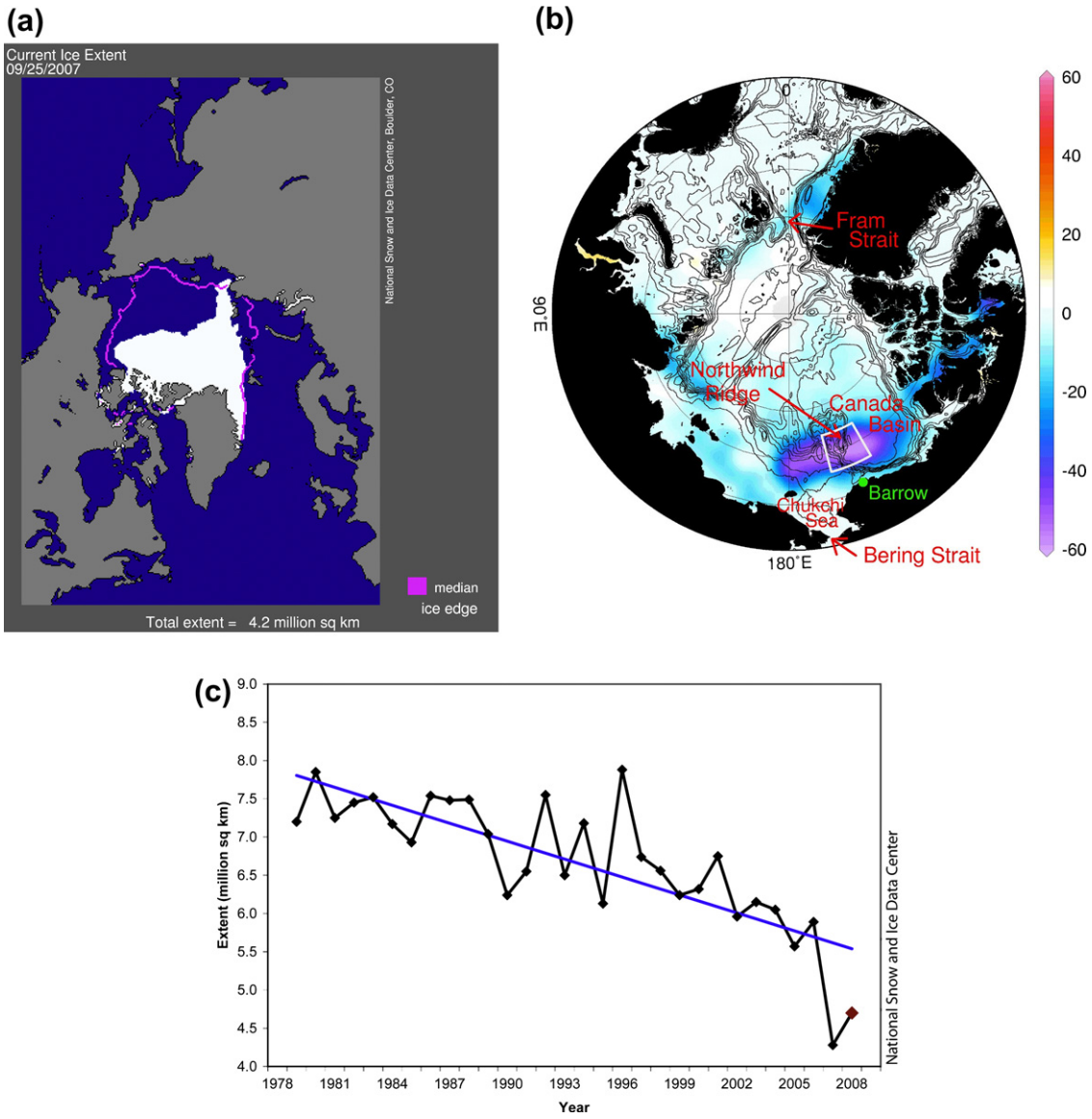

FIGURE S15.11 Arctic Ocean. (a) Sea ice extent 9/25/2007. Pink indicates the average extent for years 1979–2000. *Source: From NSIDC (2007).* (b) Sea ice concentration anomaly (%) for September 1998–2003 minus 1979–1997. *Source: From Shimada et al. (2006).* (c) Arctic sea ice extent in September (1978–2008), based on satellite microwave data. *Source: From NSIDC (2008b); after Serreze et al. (2007).*

ice there that is more likely to melt in summer. Sea ice transport in the Transpolar Drift increases with greater export through Fram Strait, even as ice moves more slowly from the Beaufort Sea across the North Pole; the Beaufort Gyre contracts and weakens (Rigor et al., 2002).

Other effects that have reduced sea ice include greater incursion of Pacific Summer Water through Bering Strait into the Beaufort Gyre from 1998 to 2003; a positive feedback in the ocean-ice-winds system has been proposed (Shimada et al., 2006). Sea ice reduction leads to a positive feedback, as the greater area of open water absorbs more heat from the sun (ice-albedo feedback).

The loss of Arctic sea ice is now faster than predicted by the ensemble of climate models in the fourth assessment report of the IPCC (2007), based on greenhouse gas forcing. It is now expected that the Arctic will be ice-free in summer within the next several decades, which is much earlier than the prediction of the end of the twenty-first century given in the IPCC report. The conclusion is that the polar-amplification of global warming is indeed operable and that the trend of sea ice loss is due to global change (Serreze et al., 2007).

S15.5.3. Variations in Nordic Seas and Arctic Water Properties

The Nordic Seas have been warming at all depths since the 1980s. This has affected and also resulted from changes in convection. Deep convection occurs in the Greenland Sea, renewing intermediate through bottom waters throughout the Nordic Seas. However, the depth and properties of convection have varied greatly. Convection reaching to the bottom is likely to have occurred in the early 1980s, but was rare enough that Carmack and Aagaard (1973) and Clarke, Swift, Reid, & Koltermann (1990) hypothesized other mechanisms for bottom water renewal (Section 12.2). Since the early 1980s, top-to-bottom convection has been replaced by annual intermediate depth convection (down to 1000–2000 m; Ronski & Budéus, 2005b; Hughes, Holliday, & Beszczynska-Möller, 2008). Because of the cessation of very deep convection, the vertical structure in the Greenland Sea has been replaced by a two-layer structure with active convection in the upper layer and older water beneath. Reduced convection in the Greenland Sea reduces the amount of carbon dioxide that can be pulled down into deep water and could boost global warming. Regardless of whether it reaches to intermediate depths or the bottom, renewal of Greenland Sea Deep Water is important for North Atlantic Deep Water formation, since this convection is still deeper than the Greenland-Scotland ridge sill depths and the renewed water can spill southward into the deep North Atlantic.

Decades long freshening throughout the Nordic Seas until the late 1990s mirrored freshening of the subpolar North Atlantic at the same time (Chapter 9). A long time series just west of the Norwegian Atlantic Current, at Ocean Weather Station Mike (66°N, 2°E), shows the freshening trend in the upper 1500 m from the mid-1970s until 1998 (Figure S15.12). However, the whole region, including the Nordic Seas and subpolar North Atlantic, started to become saltier in the late 1990s after the end of the record shown in Figure S15.12 (Hughes et al., 2008).

Within the Arctic, north of Svalbard, there has been remarkable warming in the 1990s up to the present (Figures S15.13 and S15.14). The strongest signal is warming of the Atlantic Water temperature maximum. A new pulse of warm Atlantic Water entered the Arctic in 2004, captured by the annually repeated hydrographic section in Figure S15.14 (Polyakov, personal communication, 2009), but past the end of the time series depicted in Figure S15.13. After 2004, the core temperature of the Atlantic Water layer increased by almost 2 °C in the Laptev Sea. Although this warm Atlantic layer is capped by a much colder surface layer,

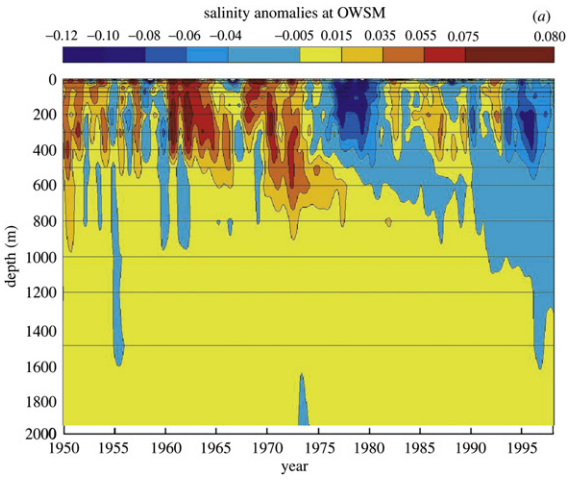

FIGURE S15.12 Salinity in the Norwegian Sea, at Ocean Weather Station Mike offshore of the Norwegian Atlantic Current (66°N, 2°E). Source: From Dickson, Curry, and Yashayaev (2003, Recent changes in the North Atlantic, Phil. Trans. Roy. Soc. A, 361, p. 1922, Fig. 2).

supported by the Arctic halocline, the warm layer is expanding upward and can represent an additional source of heat that reduces sea ice cover above it.

There are few time series that can be used to study changes over decades in the Arctic. The data sets, which are primarily Russian, are geographically sparse during some decades, and unevenly distributed in time (Swift, Aagaard, Timokhov, & Nikiforov, 2005). Likely because of the sparse data, there are two competing views of the evolution of temperature within the Atlantic Water layer, whose temperature has become something of an index of Arctic Ocean climate variability. The first view (Polyakov et al., 2005), represented in Figure S15.13a, which shows the average of temperature anomalies in all regions, suggests a multidecadal timescale, which matches the timescale of the AMO index although they are not in phase with each other. The current warming of the layer is comparable to the warming in the 1920s–1940s, with cool periods before 1920 and in the 1960s and 1970s.

The second view (Figure S15.13b from Swift et al., 2005), in which the geographic distribution of the temperature changes is retained, does not find a cool period throughout the 1960s and 1970s. Rather there was a warming in the mid to late 1960s in all regions except the Eurasian continental shelf. There was a cyclonically propagating Atlantic layer warm event in the second half of the 1950s similar to that of the 1990s. Rapid onset of Arctic-wide warmth during the 1960s was apparently followed by an equally widespread, but even longer cold period that lasted until the late 1980s. The 1950s event is obscured in Figure S15.13 because of basin-wide averaging; the rapidity of the onset of the 1960s warming is also not as apparent in Figure S15.13 as in the more comprehensive data set.

At this point it is unclear whether the present warming of the Atlantic Water layer is natural or anthropogenic, but this warming can only reinforce the present increased loss of Arctic sea ice, which does have its roots in global change.

S15.6. CLIMATE AND THE SOUTHERN OCEAN

Climate variability in the Southern Ocean is still being characterized because of the shortness of good time series. It appears to be dominated by (1) a circumpolar pattern (SAM; (Figure S15.15) and (2) higher mode patterns with large amplitude in the central Pacific sector of the Antarctic. Both have interannual and longer timescales, and are manifested in SST, circulation, and sea ice extent. ENSO (Chapter 10) has an impact on these modes, especially at interannual timescales. Longer timescales appear to be tied in part to anthropogenic change.

ENSO variability in the tropical Pacific is connected to the Southern Ocean through the atmosphere. The resulting Antarctic response to ENSO has a dipole character with the two centers in the central Pacific (Ross Sea) and the

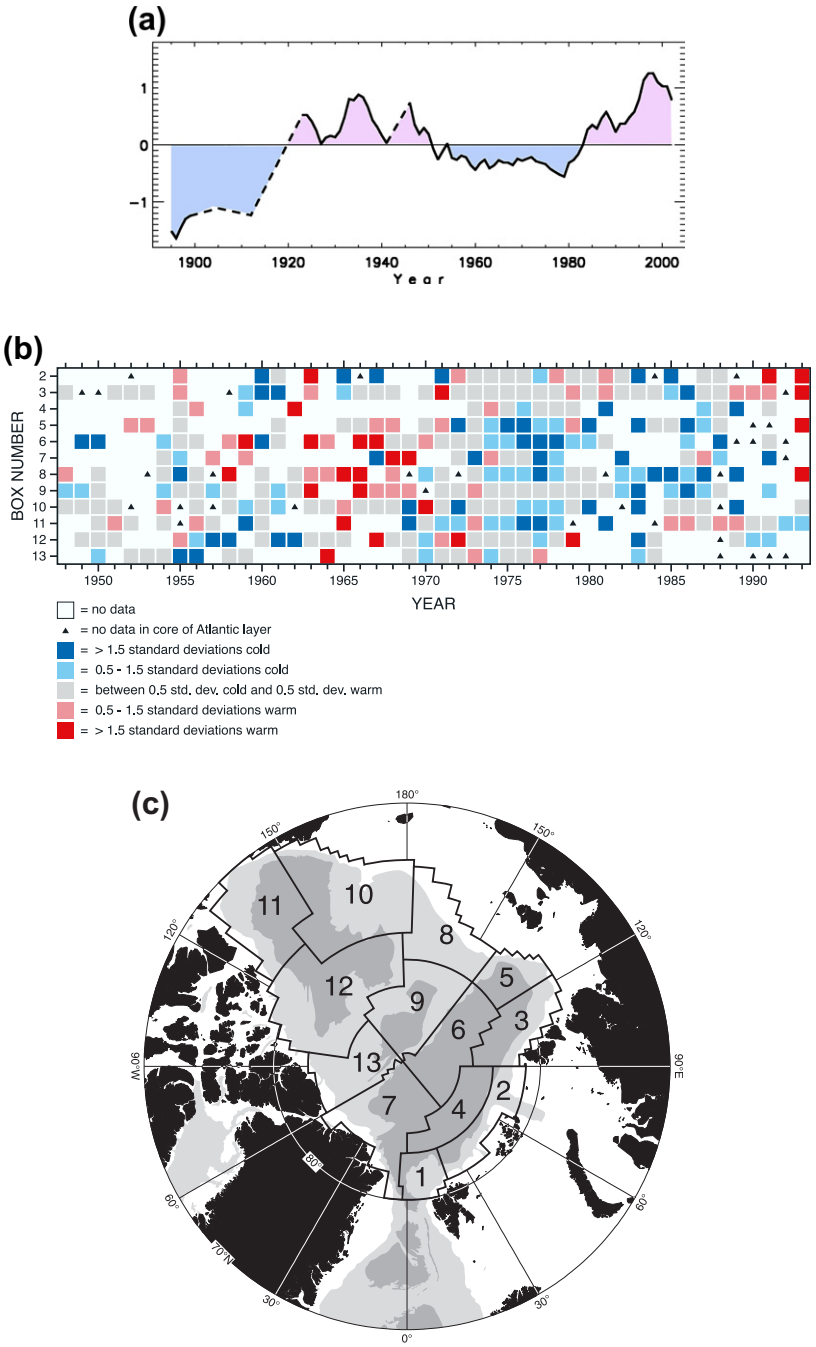

FIGURE S15.13 Atlantic Water core temperature in the Arctic Ocean: (a) Mean anomaly (°C), averaged from anomalies in ten regions relative to the mean over the record. *Source: From Polyakov et al. (2005).* (b) Variability for all geographic boxes shown in (c), leaving blank those with too few observations. *Source: From Swift et al. (2005).*

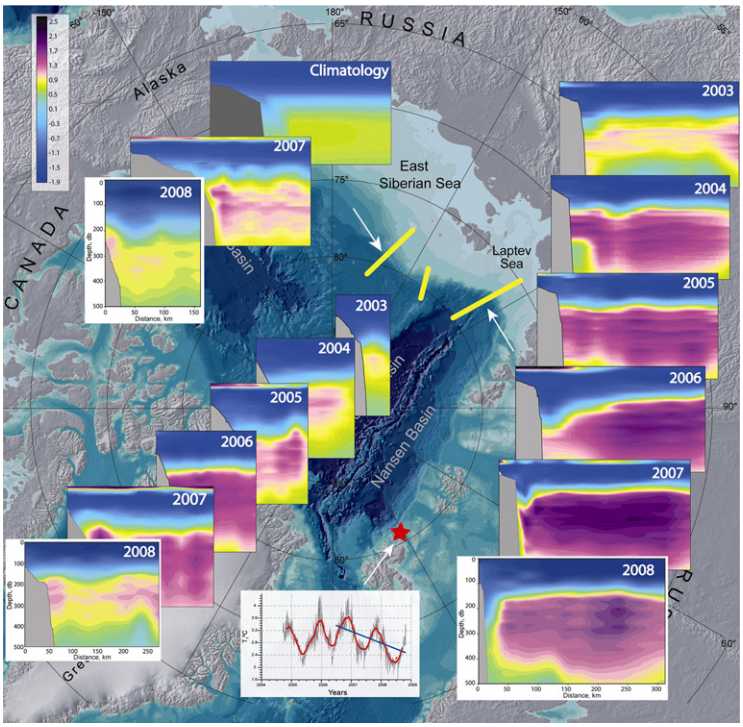

FIGURE S15.14 Arctic Ocean. Sections of potential temperature (°C) for 2003–2008, and a time series of temperature northeast of Svalbard. *(I. Polyakov, personal communication, 2009.)*

western Atlantic (Weddell Sea) out of phase with each other. ENSO warm events are associated with warm SST/reduced sea ice in the Pacific center and the opposite in the Atlantic center. La Niña cold events have the opposite response. This Antarctic Dipole has its own internal air-sea-ice feedbacks and persists for several years after being triggered by ENSO (Yuan, 2004).

The Southern Annular Mode, also known as the Antarctic Oscillation , is the dominant decadal climate mode of the Southern Hemisphere (Thompson & Wallace, 2000). It subsumes various Southern Hemisphere climate modes that were described in the 1990s. The SAM index is the amplitude of an EOF (Section 6.6.1) of the atmosphere's geopotential anomaly (similar to dynamic height; (Figure S15.15). The SAM pattern has a center of pressure of one sign over Antarctica and the opposite sign in a ring (annulus) at 40 to 50°S. Regions of greatest amplitude occur in the Ross Sea region and are of opposite sign in the southwest Pacific and central Indian Ocean. When the SAM index is positive and high, the south-north pressure difference is large (higher pressure in the red areas and lower pressure in the blue area in the figure). This means that the westerly winds are more intense. There is also a southward shift in the maximum westerlies. Its SST pattern is more complex and is related to the changes in both zonal and meridional winds. Stronger westerlies cause stronger northward Ekman transport in the (ACC), and changes in patterns of upwelling around Antarctica (Hall & Visbeck, 2002).

The SAM index had been rising noisily for over 40 years, reaching a maximum in the early 2000s, after which it began to decline (Figure S15.15). The positive SAM trend has been

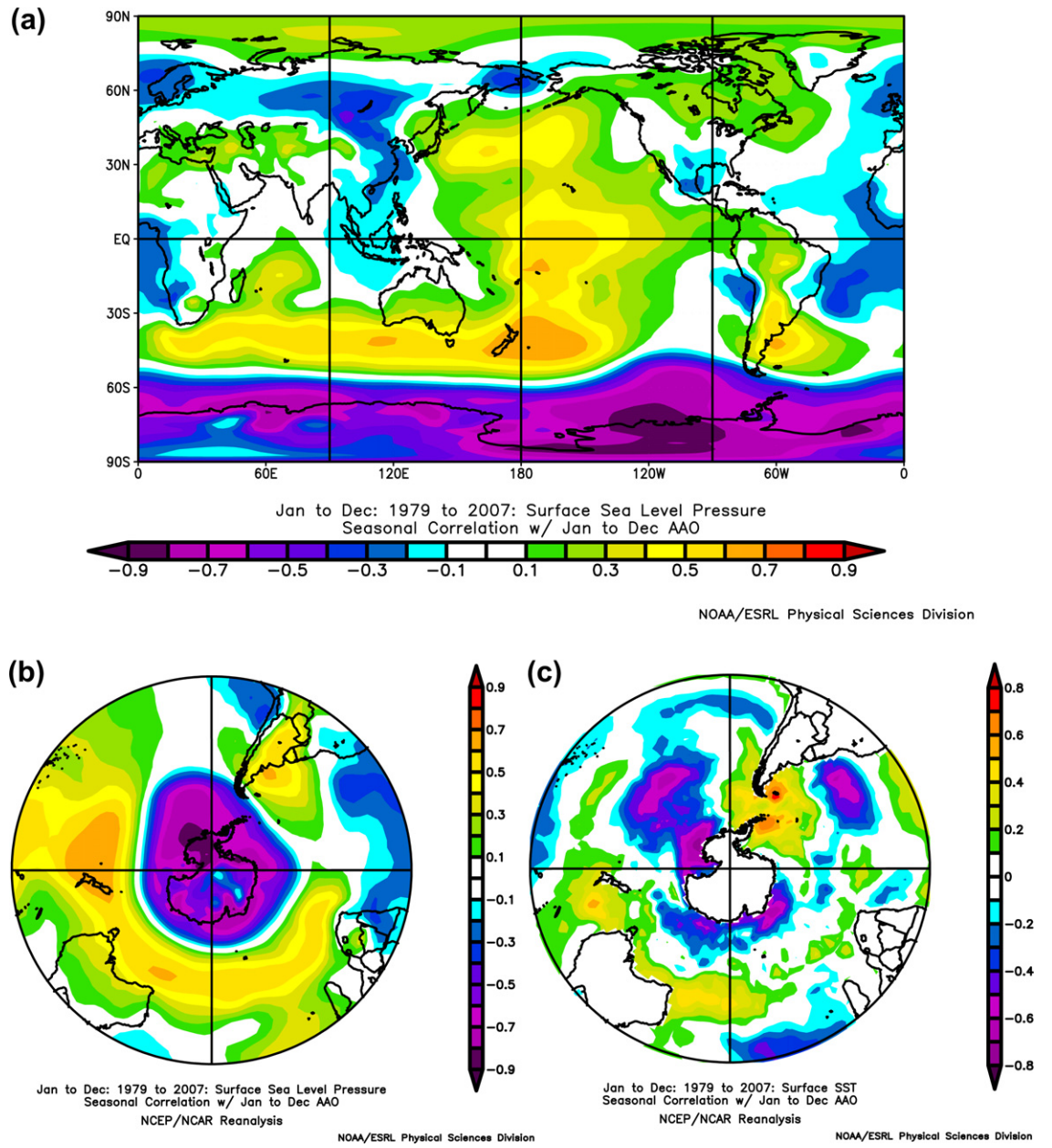

FIGURE S15.15 Southern Ocean. Correlation of the Southern Annular Mode index (*from Thompson and Wallace, 2000*), for all months from 1979 to 2005, with (a, b) sea level pressure and (c) SST. (Data and graphical interface from NOAA ESRL, 2009b.) (d) Time series of SAM index. *Source: From the IPCC AR4, Trenberth et al., 2007; Climate Change 2007: The Physical Science Basis. Working Group I Contribution to the Fourth Assessment Report of the Intergovernmental Panel on Climate Change, Figure 3.32. Cambridge University Press.)*

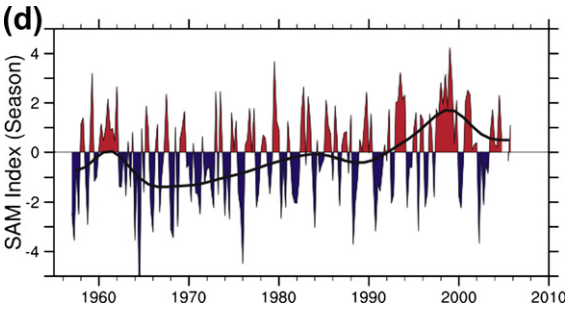

FIGURE S15.15 (*Continued*).

related to anthropogenic change (Thompson & Solomon, 2002; Marshall, 2003). The rise in SAM has been related to a southward shift and strengthening of the ACC and to an increase in subtropical circulation in the western South Pacific (Roemmich et al., 2007). The southward shift resulted in incursion of warmer waters at depth on the north side of the ACC. Such warming has been observed over the past 70 years at 900 m depth (Figure S15.16 from Gille, 2002; Fyfe, 2006). The change in the ACC might also have resulted in an increase in eddy activity, which could increase the poleward heat transport (Meredith & Hogg, 2006).

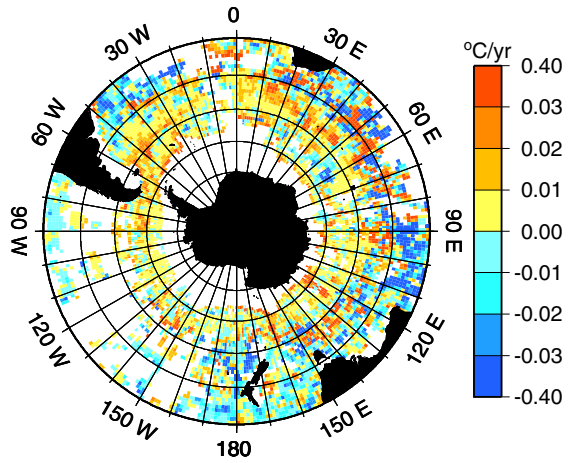

FIGURE S15.16 Temperature change at 900 m in the Southern Ocean from the 1930s to 2000, including shipboard profile and ALACE profiling float data. The largest warming occurs in the Subantarctic Zone, and a slight cooling to the north. *Source: From Gille (2002).*

S15.7. GLOBAL OCEAN CLIMATE CHANGE

Observing anthropogenic climate change using in situ observations is difficult, as its imprint is mostly sought in terms of long-term trends in a particular observed field. For the global ocean, long time series are not available in many regions, especially away from the coasts, islands, and heavily trafficked shipping lanes. Our best long time series are from tide stations at scattered sites around the globe. Our best time series with good spatial coverage are from satellites, but this coverage only began in earnest in the 1980s. Nevertheless, reconstructions of global ocean heat content, surface temperature, sea level, and near-surface salinity are of high enough quality, with quantifiable error estimates, to begin to discern unambiguous trends over many decades. When interpreted along with similar time series of atmospheric observations, and in the context of simple to complex climate models, the ocean observations provide support for concluding that there is discernible evidence for global change in response mainly to greenhouse gas forcing (IPCC, 2007).

Heat content of the upper ocean (0–700 m) has been increasing since the 1950s, with a possible decline through the 1960s (Figure S15.17). The heat content increase from 1961 to 2003 was about 16×10^{22} J. This was associated with an average temperature increase of about 0.1 °C in the upper 700 m (Levitus et al., 2005). The SST changed about 0.4 °C over that time. The heat content change is equivalent to a change in surface heat flux of about 0.4 W/m^2 (Domingues et al., 2008), which is far smaller than the error in air–sea heat flux observations, of order 10 W/m^2. Even though the task of mapping and analyzing ocean temperature is

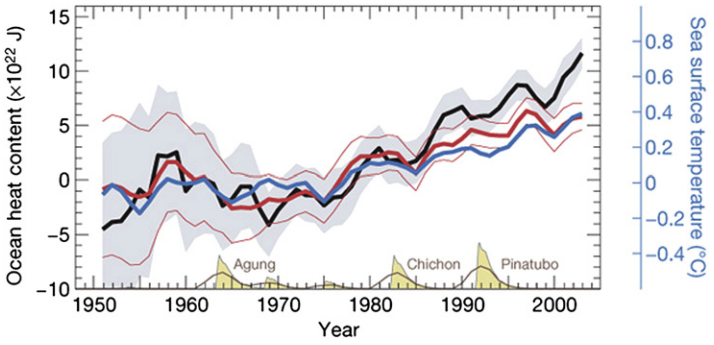

FIGURE S15.17 Global ocean heat content change ($\times 10^{22}$ J) for the upper 0–700 m (black), 0–100 m (red), and SST change (blue). One standard deviation of error is indicated in gray (for 0–700 m) and thin red lines (for 0–100 m). The optical thickness of the stratosphere is indicated at the bottom, with three major volcanoes labeled. *Source: From Domingues et al. (2008).*

formidable, it is a far more robust indicator of climate change than could ever be derived in the foreseeable future from direct observations of air–sea heat flux.

The heat content of the entire global system has increased since the 1950s. The oceans have absorbed 90% of this heat increase because there is much more heat storage capacity in water than in the atmosphere, sea and land ice, or the continents. The much greater specific heat of water compared with gas means that the 0.1 °C change in upper ocean temperature would be equivalent to an almost 100 °C change in atmospheric temperature (Levitus et al., 2005).

The spatial distribution of the ocean's heat content and SST trend over the past 50 years is not uniform (Figures S15.18 and S14.12). Climate change models predict non-uniform changes when projected over the next century, with greatest warming in the Arctic and little change in the subpolar North Atlantic and ACC (IPCC, 2007). Observed warming is widespread and is indeed more exaggerated in the Arctic where sea ice cover has been retreating significantly (Chapter 12). Heat content appears to have decreased in the subpolar North Pacific and North Atlantic and in the Pacific's tropical warm pool. SST trends (Figure S15.18) differ somewhat from water column heat content, showing warming in the warm pool, and also a band of cooling along the ACC in the region where air–sea fluxes warm the ocean in the annual mean (Figure 5.15 and S5.9). This band is associated with wind-driven upwelling, which can decrease SST. An increased AAO (SAM) index for the 1950s through 2000 (Marshall, 2003) lowered sea level pressure and strengthened westerly winds and upwelling, which could have decreased the surface temperature.

Warming has been mostly confined to the upper ocean (Figure S15.19; Levitus et al., 2005). The tropical cooling in the world average derives from the tropical Pacific and is due to an ENSO signal (Section 10.8). The subpolar Northern Hemisphere cooling is from the Atlantic (Section S15.2.4). Details for each of the ocean basins were described in the basin chapters (9–13) and are not repeated here.

Abyssal and bottom temperatures have also been increasing worldwide based on highly accurate observations from research ships (Kawano et al., 2006, 2010; Purkey & Johnson, 2010). The changes are small, but within the uncertainty of the observations. The largest changes are found near the obvious sources of deep water. Changes that are far downstream from these sources, such as in the deep North Pacific where bottom water is hundreds of years old, can result from adjustment of the deep circulation such that the whole complex of waters shifts northward without having to advect warmer water all the way from the distant source (Nakano & Suginohara, 2002).

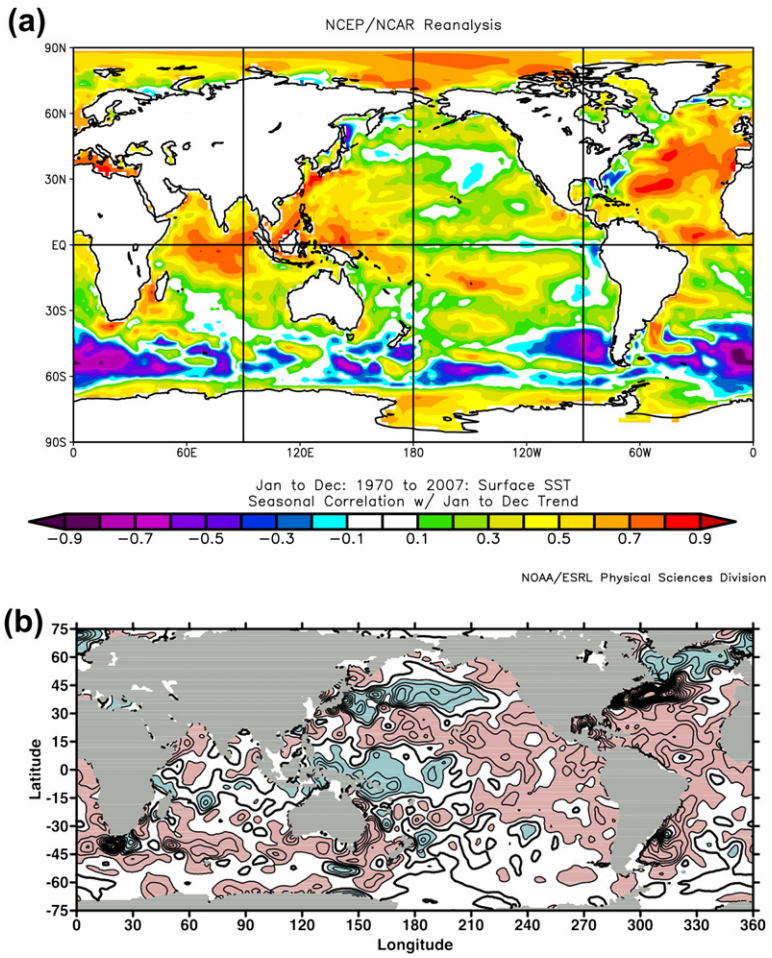

FIGURE S15.18 (a) Correlation of SST for 1970–2007 with a linear trend, based on the NCEP/NCAR reanalysis. Positive correlation means warming and negative correlation means cooling. (Data and graphical interface from NOAA ESRL, 2009b.) (b) Linear trend of change in ocean heat content per unit surface area (W m^{-2}) for the 0 to 700 m layer from 1955 to 2003, based on Levitus et al. (2005). Red shading is values above 0.25 W m^{-2} and blue shading is below −0.25 W m^{-2}. *Source: From the IPCC AR4, Bindoff et al., 2007; Climate Change 2007: The Physical Science Basis. Working Group I Contribution to the Fourth Assessment Report of the Intergovernmental Panel on Climate Change, Figure 5.2. Cambridge University Press.*

Large-scale but weak trends in upper ocean salinity from 1955 to 1998 have been demonstrated (Figure S15.20 from Boyer et al., 2005, and more recent results from Durack & Wijffels, 2010). These represent a redistribution of freshwater, rather than a net change in freshwater content. The average ocean salinity should change (decrease) in response to net melting of land ice, which is an expected result of global warming. A quick calculation of the impact of such melt shows that detection is feasible if the meltoff is large enough. However, at this time, such a change in average ocean salinity has not been observed. There has been a weak increase in Atlantic and Indian Ocean salinity and a decrease in Pacific Ocean salinity. This is suggestive of an increase in the cycle of precipitation and evaporation. This could result from warming of the atmosphere, which increases its capacity to hold water and hence cycle it in greater amounts from evaporation regions to precipitation regions (Bindoff et al., 2007; Talley, 2008).

Global mean sea level has increased over the 130 years of reconstructed records (Figure S15.21). Uncertainties in this reconstruction are

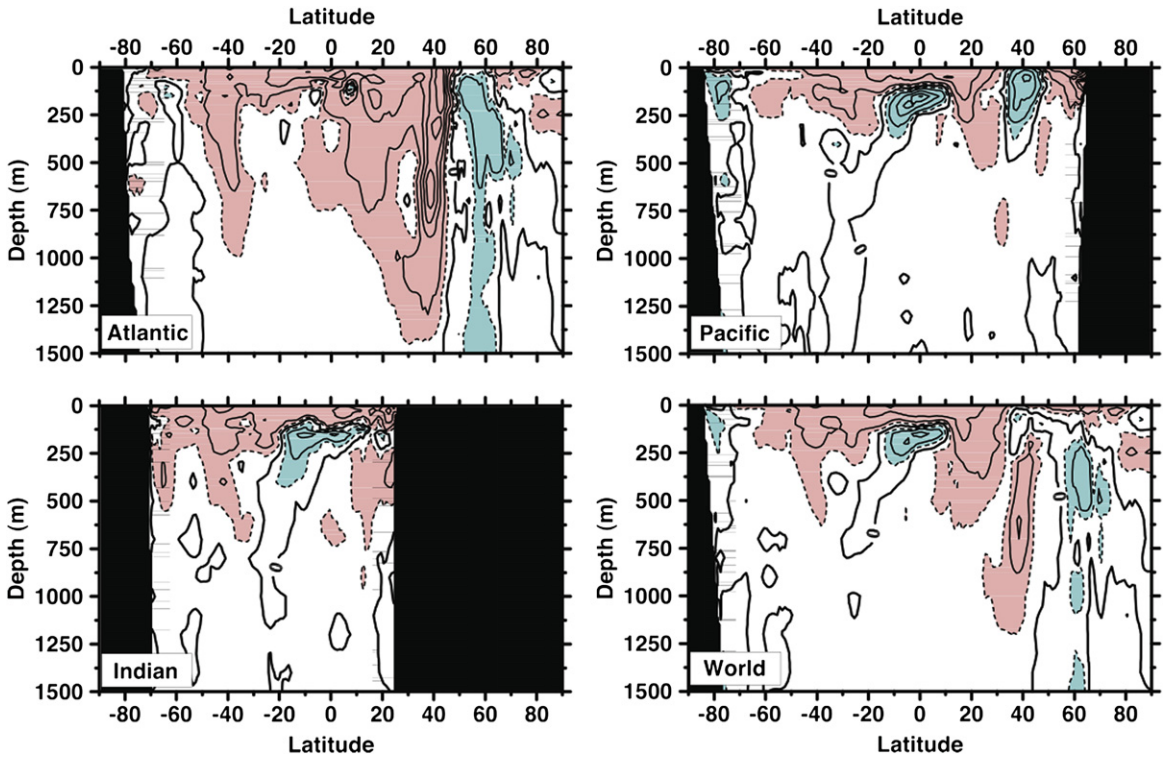

FIGURE S15.19 Zonally averaged linear temperature trend for 1955 to 2003 (contour interval of 0.05°C per decade) for the world ocean. Pink: increasing trend. Blue: decreasing trend. *Source: From the IPCC AR4, Bindoff et al., 2007; Climate Change 2007: The Physical Science Basis. Working Group I Contribution to the Fourth Assessment Report of the Intergovernmental Panel on Climate Change, Figure 5.3. Cambridge University Press.*

large, but the increasingly accurate data sets of recent decades show the same increasing trend. Since 1961, which begins a period of improved data coverage, the average rate has been about 2 mm/year. Since 1993, with even better observations, it has been about 3 mm/year (Bindoff et al., 2007). About half of the sea level increase since 1993 can be attributed to changes in thermal expansion due to the warming ocean and half to glacier and ice cap/ice sheet melting. Similar to changes in ocean heat content, there is large-scale spatial variation in the sea level change, as can be expected from the large contribution of thermal expansion to sea level change.

The ocean's chemical constituents have also been changing. Much attention is focused on changes in carbon parameters, since the ocean is a sink for excess anthropogenic carbon dioxide (Sabine et al., 2004), such that the ability to quantify the ocean's uptake of excess CO_2 is important for future projections of climate change. Increasing the amount of CO_2 dissolved in the ocean also increases the ocean's acidity, which is also receiving wide attention (Feely et al., 2004; National Research Council, 2010). Because this text provides no background on the complexities of the ocean's carbon budget, these changes are beyond the scope of this book.

The ocean's oxygen distribution is also changing. Oxygen and nutrient changes are mostly measured from infrequent research ship reoccupations of long sections. From such

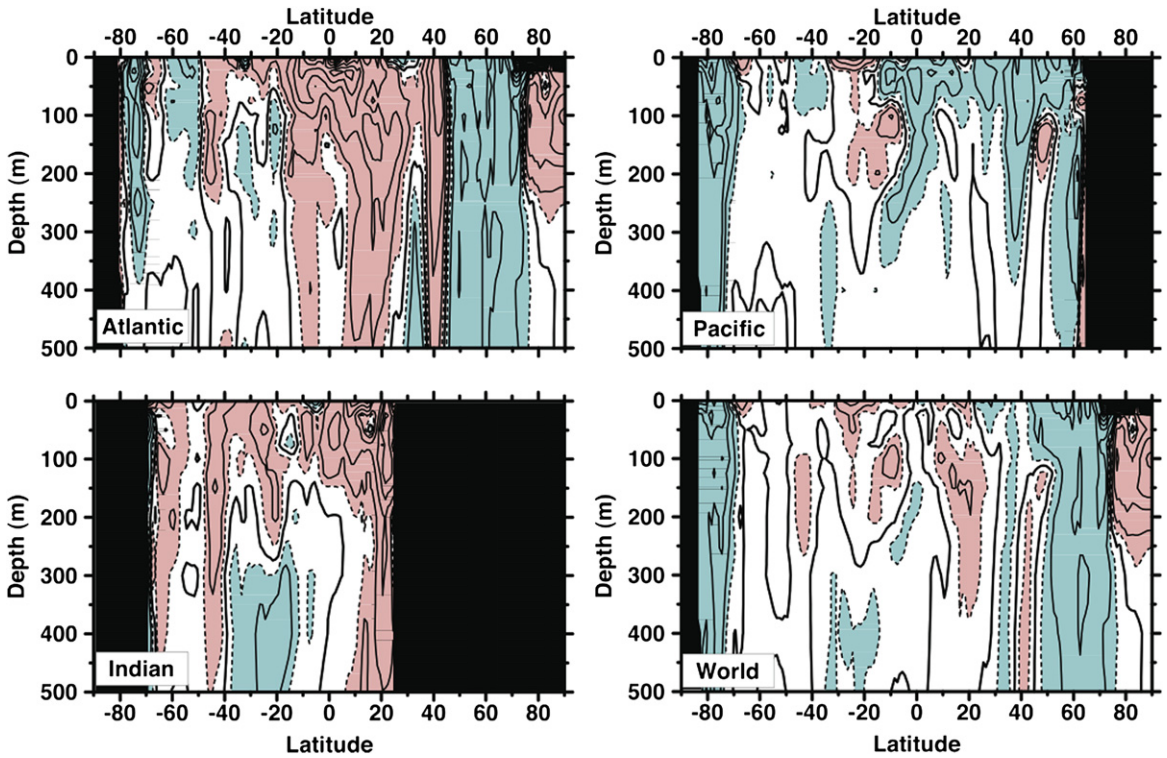

FIGURE S15.20 Zonally averaged linear salinity trend for 1955 to 2003 (contour interval of 0.01 psu per decade) for the world ocean. Pink: increasing trend. Blue: decreasing trend. *Source: From the IPCC AR4, Bindoff et al., 2007; Climate Change 2007: The Physical Science Basis. Working Group I Contribution to the Fourth Assessment Report of the Intergovernmental Panel on Climate Change, Figure 5.5. Cambridge University Press.*

observations, oxygen at the base of the pycnocline has declined at mid to high latitudes over the past several decades. In the northern and subtropical North Pacific, the changes are widespread and have been attributed to changes in ocean circulation and in the winter surface outcrop densities (Deutsch et al., 2005). In the northeastern North Atlantic, similar oxygen declines have been similarly attributed (Johnson & Gruber, 2007). As the ocean surface warms, the outcropping isopycnals in the circulation also shift. In subtropical gyres, the ventilated isopycnals become less dense. This leads to reduced oxygen on the underlying isopycnals that would have been vigorously ventilated in previous decades. In the Southern Ocean oxygen declines in the pycnocline in the ACC have been observed (Aoki, Bindoff, & Church, 2005). In the tropics the great oxygen minima of the denitrification regions of the upper ocean have been expanding (Stramma et al., 2008).

Thus we see that over the past several decades the ocean has been warming; its salinity has been redistributed in a manner consistent with a warmer, more humid atmosphere; sea level has been rising in response to ocean warming and land ice melt; and oxygen in the upper ocean may be declining.

Are these signals indicative of climate change? Two major issues are that the data sets are not optimized for global spatial coverage or continuous temporal coverage,

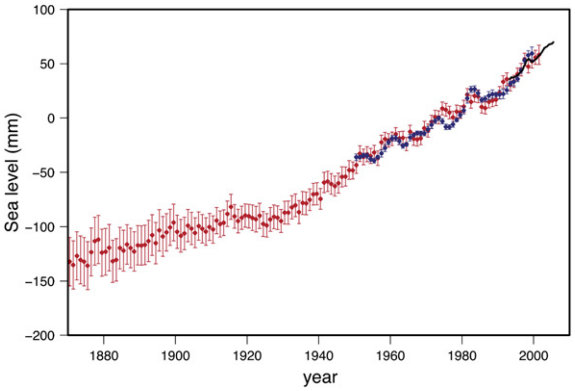

FIGURE S15.21 Global mean sea level (mm) relative to the 1961−1990 average, with 90% confidence intervals, based on sparse tide gauges (red), coastal tide gauges (blue), and satellite altimetry (black solid). *Source: From the IPCC AR4, Bindoff et al., 2007; Climate Change 2007: The Physical Science Basis. Working Group I Contribution to the Fourth Assessment Report of the Intergovernmental Panel on Climate Change, Figure 5.13. Cambridge University Press.*

and interpretation in terms of climate change is usually based on fitting linear trends to time series. The data sets have become much better in recent years, confirming the long-term trends or providing much more information for understanding the observed trends.

But even if the data coverage was perfect, trend fitting is subject to two problems: the natural climate state at the end points of the time series, and interpretation of the signal as a trend rather than part of a longer term climate variation. Thus to distinguish between natural and anthropogenic climate variability, "attribution" studies are useful. Barnett et al. (2005) approached this by examining how natural climate variability in terms of modes (Table S15.1), volcanic activity, and solar activity affect regional changes in upper ocean temperature in an ocean model. Locally, anthropogenic climate change is not necessarily distinguishable from natural variability. But when averaged over very large regions, essentially entire ocean basins, in order to obtain robust results (90% confidence level), Barnett et al. (2005) showed that the observed pattern of temperature change is inconsistent with variability arising from natural sources alone, therefore the ocean shows an imprint of global change.

References

Annamalai, H., Xie, S.P., McCreary, J.P., Murtugudde, R., 2005. Impact of Indian Ocean sea surface temperature on developing El Niño. J. Clim. 18, 302−319.

Aoki, S., Bindoff, N.L., Church, J.A., 2005. Interdecadal water mass changes in the Southern Ocean between 30E and 160E. Geophys. Res. Lett. 32 doi:10.1029/2004GL022220.

Barnett, T.P., Pierce, D.W., AchutaRao, K., Gleckler, P., Santer, B., Gregory, J., Washington, W., 2005. Penetration of human-induced warming into the World's Oceans. Science 309, 284−287.

Barnston, A.G., Livezey, R.E., 1987. Classification, seasonality and persistence of low-frequency atmospheric circulation patterns. Mon. Weather Rev. 115, 1083−1126.

Belkin, I.M., 2004. Propagation of the "Great Salinity Anomaly" of the 1990s around the northern North Atlantic. Geophys. Res. Lett. 31 L08306. doi:10.1029/2003GL019334.

Bindoff, N.L., McDougall, T.J., 2000. Decadal changes along an Indian Ocean section at 32 degrees S and their interpretation. J. Phys. Oceanogr. 30, 1207−1222.

Bindoff, N.L., Willebrand, J., Artale, V., Cazenave, A., Gregory, J., Gulev, S., Hanawa, K., Le Quere, C., Levitus, S., Nojiri, Y., Shum, C.K., Talley, L.D., Unnikrishnan, A., 2007. Observations: Oceanic climate change and sea level. In: Solomon, S., Qin, D., Manning, M., Chen, Z., Marquis, M., Averyt, K.B., Tignor, M., Miller, H.L. (Eds.), Climate Change 2007: The Physical Science Basis. Contribution of Working Group I to the Fourth Assessment Report of the Intergovernmental Panel on Climate Change. Cambridge University Press, Cambridge, UK and New York.

Bourlès, B., Lumpkin, R., McPhaden, M.J., Hernandez, F., Nobre, P., Campos, E., Yu, L., Planton, S., Busalacchi, A., Moura, A.D., Servain, J., Trotte, J., 2008. The Pirata program: History, accomplishments, and future directions. B. Am. Meteorol. Soc. 89, 1111−1125.

Boyer, T.P., Antonov, J.I., Levitus, S., Locarnini, R., 2005. Linear trends of salinity for the world ocean: 1955−1998. Geophys. Res. Lett. 32 L01604. doi:1029/2004GL021791.

Broecker, W.S., 1998. Paleocean circulation during the last deglaciation: A bipolar seesaw? Paleoceanography 13, 119−121.

Bryden, H.L., Longworth, H.R., Cunningham, S.A., 2005b. Slowing of the Atlantic meridional overturning circulation at 26.5°N. Nature 438, 655−657.

Carmack, E., Aagaard, K., 1973. On the deep water of the Greenland Sea. Deep-Sea Res. 20, 687–715.

Cayan, D.R., 1992. Latent and sensible heat flux anomalies over the northern oceans: Driving the sea surface temperature. J. Phys. Oceanogr. 22, 859–881.

Chang, P., Ji, L., Li, H., 1997. A decadal climate variation in the tropical Atlantic Ocean from thermodynamic air-sea interactions. Nature 385, 516–518.

Chiang, J.C.H., Vimont, D.J., 2004. Analogous Pacific and Atlantic meridional modes of tropical atmosphere–ocean variability. J. Clim. 17, 4143–4158.

Clark, C.O., Webster, P.J., Cole, J.E., 2003. Interdecadal variability of the relationship between the Indian Ocean zonal mode and East African coastal rainfall anomalies. J. Clim. 16, 548–554.

Clarke, R.A., Swift, J.H., Reid, J.L., Koltermann, K.P., 1990. The formation of Greenland Sea Deep Water: Double diffusion or deep convection? Deep-Sea Res. Part A 37, 1385–1424.

Cunningham, S.A., Kanzow, T., Rayner, D., Baringer, M.O., Johns, W.E., Marotzke, J., Longworth, H.R., Grant, E.M., Hirschi, J.J.-M., Beal, L.M., Meinen, C.S., Bryden, H.L., 2007. Temporal variability of the Atlantic meridional overturning circulation at 26.5°N. Science 317, 935–938.

Curry, R., Dickson, B., Yashayaev, I., 2003. A change in the freshwater balance of the Atlantic Ocean over the past four decades. Nature 426, 826–829.

Curry, R.G., McCartney, M.S., 2001. Ocean gyre circulation changes associated with the North Atlantic Oscillation. J. Phys. Oceanogr. 31, 3374–3400.

Davis, R.E., 1976. Predictability of sea surface temperature and sea level pressure anomalies over the North Pacific. J. Phys. Oceanogr. 6, 249–266.

Delworth, T.L., Mann, M.E., 2000. Observed and simulated multidecadal variability in the northern hemisphere. Clim. Dynam. 16, 661–676.

Dengler, M., Quadfasel, D., Schott, F., Fischer, J., 2002. Abyssal circulation in the Somali Basin. Deep-Sea Res. II 49, 1297–1322.

Deser, C., Holland, M., Reverdin, G., Timlin, M., 2002. Decadal variations in Labrador Sea ice cover and North Atlantic sea surface temperatures. J. Geophys. Res. 107, 3035. doi:10.1029/2000JC000683.

Deser, C., Phillips, A.S., Hurrell, J.W., 2004. Pacific interdecadal climate variability: Linkages between the tropics and the North Pacific during boreal winter since 1900. J. Clim. 17, 3109–3124.

Deutsch, C., Emerson, S., Thompson, L., 2005. Fingerprints of climate change in North Pacific oxygen. Geophys. Res. Lett. 32 L16604. doi:10.1029/2005GL023190.

Di Lorenzo, E., Schneider, N., Cobb, K.M., Franks, P.J.S., Chhak, K., Miller, A.J., McWilliams, J.C., Bograd, S.J., Arango, H., Curchitser, E., Powell, T.M., Rivière, P., 2008. North Pacific Gyre Oscillation links ocean climate and ecosystem change. Geophys. Res. Lett. 35 L08607. doi:10.1029/2007GL032838.

Dickson, R., Lazier, J., Meincke, J., Rhines, P., Swift, J., 1996. Long-term coordinated changes in the convective activity of the North Atlantic. Progr. Oceanogr. 38, 241–295.

Dickson, R., Yashayaev, I., Meincke, J., Turrell, B., Dye, S., Holfort, J., 2002. Rapid freshening of the deep North Atlantic Ocean over the past four decades. Nature 416, 832–837.

Dickson, R.R., Curry, R., Yashayaev, I., 2003. Recent changes in the North Atlantic. Phil. Trans. Roy. Soc. A 361, 1917–1933.

Dickson, R.R., Meincke, J., Malmberg, S.-A., Lee, A.J., 1988. The "Great Salinity Anomaly" in the northern North Atlantic 1968–1982. Progr. Oceanogr. 20, 103–151.

Domingues, C.M., Church, J.A., White, N.J., Gleckler, P.J., Wijffels, S.E., Barker, P.M., Dunn, J.R., 2008. Improved estimates of upper-ocean warming and multidecadal sea-level rise. Nature 453, 1090–1093.

Durack, P.J., Wijffels, S.E., 2010. Fifty-year trends in global ocean salinities and their relationship to broad-scale warming. J. Clim. 23, 4342–4362.

Enfield, D., Mestas-Nuñez, A., Trimble, P., 2001. The Atlantic Multidecadal Oscillation and its relation to rainfall and river flows in the continental U.S. Geophys. Res. Lett. 28, 2077–2080.

Feely, R.A., Sabine, C.L., Lee, K., Berelson, W., Kleypas, J., Fabry, V.J., Millero, F.J., 2004. Impact of anthropogenic CO_2 on the $CaCO_3$ system in the oceans. Science 305, 362–366.

Flatau, M.K., Talley, L.D., Niiler, P.P., 2003. The North Atlantic Oscillation, surface current velocities, and SST changes in the subpolar North Atlantic. J. Clim. 16, 2355–2369.

Fowler, C., Emery, W.J., Maslanik, J., 2004. Satellite-derived evolution of Arctic sea ice age: October 1978 to March 2003. IEEE Remote Sensing Lett. 1, 71–74.

Fyfe, J.C., 2006. Southern Ocean warming due to human influence. Geophys. Res. Lett. 33 L19701. doi:10.1029/2006GL027247.

Gille, S.T., 2002. Warming of the Southern Ocean since the 1950s. Science 295, 1275–1277.

Girton, J.B., Pratt, L.J., Sutherland, D.A., Price, J.F., 2006. Is the Faroe Bank Channel overflow hydraulically controlled? J. Phys. Oceanogr. 36, 2340–2349.

Häkkinen, S., Rhines, P.B., 2004. Decline of subpolar North Atlantic circulation during the 1990s. Science 304, 555–559.

Hall, A., Visbeck, M., 2002. Synchronous variability in the southern hemisphere atmosphere, sea ice and ocean resulting from the annular mode. J. Clim. 15, 3043–3057.

Hughes, S.L., Holliday, N.P., Beszczynska-Möller, A. (Eds.), 2008. ICES Report on Ocean Climate 2007. ICES Cooperative Research Report No. 291, p. 64. http://www.noc.soton.ac.uk/ooc/ICES_WGOH/iroc.php (accessed 7.1.09).

Hurrell, J., 1995. Decadal trends in the North Atlantic Oscillation: Regional temperatures and precipitation. Science 269, 676–679.

Hurrell, J., 2009. Climate Indices. NAO Index Data provided by the Climate Analysis Section, NCAR, Boulder, Colorado (Hurrell, 1995). http://www.cgd.ucar.edu/cas/jhurrell/nao.stat.winter.html (accessed 6.23.09).

Hurrell, J.W., Kushnir, Y., Ottersen, G., Visbeck, M., 2003. An overview of the North Atlantic Oscillation. In: The North Atlantic Oscillation: Climate Significance and Environmental Impact. Geophys. Monogr. Ser. 134, 1–35.

Ihara, C., Kushnir, Y., Cane, M.A., 2008. Warming trend of the Indian Ocean SST and Indian Ocean dipole from 1880 to 2004. J. Clim. 21, 2035–2046.

IPCC, 2007. Summary for Policymakers. In: Solomon, S., Qin, D., Manning, M., Chen, Z., Marquis, M., Averyt, K.B., Tignor, M., Miller, H.L. (Eds.), Climate Change 2007: The Physical Science Basis. Contribution of Working Group I to the Fourth Assessment Report of the Intergovernmental Panel on Climate Change. Cambridge University Press, Cambridge, UK, New York.

Jin, F.F., 1996. Tropical ocean-atmosphere interaction, the Pacific cold tongue, and the El Niño-Southern Oscillation. Science 274, 76–78.

JISAO, 2004. Arctic Oscillation (AO) time series, 1899 — June 2002. JISAO. http://www.jisao.washington.edu/ao/ (accessed 3.18.10).

Johannessen, O.M., Shalina, E.V., Miles, M.W., 1999. Satellite evidence for an arctic sea ice cover in transformation. Science 286, 1937–1939.

Johnson, G.C., Gruber, N., 2007. Decadal water mass variations along 20°W in the northeastern Atlantic Ocean. Progr. Oceanogr. 73, 277–295.

Josey, S.A., Marsh, R., 2005. Surface freshwater flux variability and recent freshening of the North Atlantic in the eastern subpolar gyre. J. Geophys. Res. 110 C05008. doi:10.1029/2004JC002521.

Kaplan, A., Cane, M., Kushnir, Y., Clement, A., Blumenthal, M., Rajagopalan, B., 1998. Analyses of global sea surface temperature 1856–1991. J. Geophys. Res. 103, 18567–18589.

Kawano, T., Doi, T., Uchida, H., Kouketsu, S., Fukasawa, M., Kawai, Y., Katsumata, K., 2010. Heat content change in the Pacific Ocean between 1990s and 2000s. Deep-Sea Res. II 57, 1141–1151.

Kawano, T., Fukasawa, M., Kouketsu, S., Uchida, H., Doi, T., Kaneko, I., Aoyama, M., Schneider, W., 2006. Bottom water warming along the pathway of Lower Circumpolar Deep Water in the Pacific Ocean. Geophys. Res. Lett. 33 L23613. doi:10.1029/2006GL027933.

Klein, B., Roether, W., Manca, B.B., Bregant, D., Beitzel, V., Kovacevic, V., Luchetta, A., 1999. The large deep water transient in the Eastern Mediterranean. Deep-Sea Res. I 46, 371–414.

Klein, S.A., Soden, B.J., Lau, N.C., 1999. Remote sea surface temperature variations during ENSO: Evidence for a tropical atmospheric bridge. J. Clim. 12, 917–932.

Krishnamurthy, V., Kirtman, B.P., 2003. Variability of the Indian Ocean: relation to monsoon and ENSO.Q.J. Roy. Meteorol. Soc. 129, 1623–1646.

Kushnir, Y., Seager, R., Miller, J., Chiang, J.C.H., 2002. A simple coupled model of tropical Atlantic decadal climate variability. Geophys. Res. Lett. 29, 23. doi:10.1029/2002GL015874.

Levitus, S., Antonov, J.I., Boyer, T.P., 2005. Warming of the world Ocean, 1955–2003. Geophys. Res. Lett. 32 L02604. doi:10.1029/2004GL021592.

Macrander, A., Send, U., Valdimarsson, H., Jónsson, S., Käse, R.H., 2005. Interannual changes in the overflow from the Nordic Seas into the Atlantic Ocean through Denmark Strait. Geophys. Res. Lett. 32 L06606. doi:10.1029/2004GL021463.

Madden, R., Julian, P., 1994. Observations of the 40-50 day tropical oscillation: A review. Mon. Weather Rev. 112, 814–837.

Mantua, N.J., Hare, S.R., Zhang, Y., Wallace, J.M., Francis, R.C., 1997. A Pacific interdecadal climate oscillation with impacts on salmon production. B. Am. Meteor. Soc. 78, 1069–1079.

Marshall, G., 2003. Trends in the Southern Annular Mode from observations and reanalyses. J. Clim. 16, 4134–4143.

Martinson, D.G., Steele, M., 2001. Future of the Arctic sea ice cover: Implications of an Antarctic analog. Geophys. Res. Lett. 28, 307–310.

Maslanik, J., Serreze, M., Agnew, T., 1999. On the record reduction in 1998 western Arctic sea-ice cover. Geophys. Res. Lett. 26, 1905–1908.

McDonagh, E.L., Bryden, H.L., King, B.A., Sanders, R.J., Cunningham, S.A., Marsh, R., 2005. Decadal changes in the south Indian Ocean thermocline. J. Clim. 18, 1575–1590.

Meredith, M.P., Hogg, A.M., 2006. Circumpolar response of Southern Ocean eddy activity to a change in the Southern Annular Mode. Geophys. Res. Lett. 33 L16608. doi:10.1029/2006GL026499.

Molinari, R.L., Fine, R.A., Wilson, W.D., Curry, R.G., Abell, J., McCartney, M.S., 1998. The arrival of recently formed Labrador Sea Water in the Deep Western Boundary Current at 26.5°N. Geophys. Res. Lett. 25, 2249–2252.

Nakano, H., Suginohara, N., 2002. Importance of the eastern Indian Ocean for the abyssal Pacific. J. Geophys. Res. 107 (C12) doi:10.1029/2001JC001065.

National Research Council, 2010. Ocean acidification: A national strategy to meet the challenges of a changing ocean. National Academies Press, Washington D.C. pp 152.

NOAA CPC, 2005. Madden/Julian Oscillation (MJO). NOAA/National Weather Service. http://www.cpc.ncep.noaa.gov/products/precip/CWlink/MJO/mjo.shtml (accessed 12.28.09).

NOAA ESRL, 2009b. Linear correlations in atmospheric seasonal/monthly averages. NOAA Earth System Research Laboratory Physical Sciences Division. http://www.cdc.noaa.gov/data/correlation/ (accessed 10.30.09).

NSIDC, 2007. Arctic sea ice news fall 2007. National Snow and Ice Data Center. http://nsidc.org/arcticseaicenews/2007.html (accessed 3.17.09).

NSIDC, 2008b. Arctic sea ice down to second-lowest extent; likely record-low volume. National Snow and Ice Data Center. http://nsidc.org/news/press/20081002_seaice_pressrelease.html (accessed 3.17.09).

NSIDC, 2009b. Arctic climatology and meteorology primer. National Snow and Ice Data Center. http://nsidc.org/arcticmet/ (accessed 3.1.09).

Olsen, S.M., Hansen, B., Quadfasel, D., Østerhus, S., 2008. Observed and modeled stability of overflow across the Greenland-Scotland ridge. Nature 455, 519–523.

Polyakov, I.V., 22 co-authors, 2005. One more step toward a warmer Arctic. Geophys. Res. Lett. 32 L17605. doi:10.1029/2005GL023740.

Proshutinsky, A.Y., Johnson, M.A., 1997. Two circulation regimes of the wind-driven Arctic Ocean. J. Geophys. Res. 102, 12493–12514.

Purkey, S.G., Johnson, G.C., 2010. Antarctic bottom water warming between the 1990s and 2000s: Contributions to global heat and sea level rise budgets. J. Clim. 23, 6336–6351.

Reverdin, G., Durand, F., Mortensen, J., Schott, F., Valdimarsson, H., 2002. Recent changes in the surface salinity of the North Atlantic subpolar gyre. J. Geophys. Res. 107 (C12) doi:10.1029/2001JC001010.

Rigor, I.G., Wallace, J.M., Colony, R.L., 2002. Response of sea ice to the Arctic Oscillation. J. Clim. 15, 2648–2663.

Roemmich, D., Gilson, J., Davis, R., Sutton, P., Wijffels, S., Riser, S., 2007. Decadal spin-up of the South Pacific subtropical gyre. J. Phys. Oceanogr. 37, 162–173.

Ronski, S., Budéus, G., 2005b. Time series of winter convection in the Greenland Sea. J. Geophys. Res. 110 C04015. doi:10.1029/2004JC002318.

Rothrock, D., Yu, Y., Maykut, G., 1999. Thinning of the Arctic sea-ice cover. Geophys. Res. Lett. 26, 3469–3472.

Sabine, C.L., Feely, R.A., Gruber, N., Key, R.M., Lee, K., Bullister, J.L., Wanninkhof, R., Wong, C.S., Wallace, D.W.R., Tilbrook, B., Millero, F.J., Peng, T.-H., Kozyr, A., Ono, T., Rios, A.F., 2004. The oceanic sink for anthropogenic CO_2. Science 305, 367–371.

Saji, N.H., Goswami, B.N., Vinayachandran, P.N., Yamagata, T., 1999. A dipole mode in the tropical Indian Ocean. Nature 401, 360–363.

Schneider, N., Cornuelle, B.D., 2005. The forcing of the Pacific Decadal Oscillation. J. Clim. 18, 4355–4373.

Schott, F.A., McCreary Jr., J., 2001. The monsoon circulation of the Indian Ocean. Progr. Oceanogr. 51, 1–123.

Schott, F.A., Stramma, L., Giese, B.S., Zantopp, R., 2009. Labrador Sea convection and subpolar North Atlantic Deep Water export in the SODA assimilation model. Deep-Sea Res. I 56, 926–938.

Serreze, M.C., Holland, M.M., Stroeve, J., 2007. Perspectives on the Arctic's shrinking sea-ice cover. Science 16, 1533–1536.

Shimada, K., Kamoshida, T., Itoh, M., Nishino, S., Carmack, E.C., McLaughlin, F., Zimmerman, S., Proshutinsky, A., 2006. Pacific Ocean Inflow: Influence on catastrophic reduction of sea ice cover in the Arctic Ocean. Geophys. Res. Lett. 33 L08605. doi; 10.1029/2005GL025624.

Steele, M., Morison, J., Ermold, W., Rigor, I., Ortmeyer, M., Shimada, K., 2004. Circulation of summer Pacific halocline water in the Arctic Ocean. J. Geophys. Res. 109 C02027. doi:10.1029/2003JC002009.

Stramma, L., Johnson, G.C., Sprintall, J., Mohrholz, V., 2008. Expanding oxygen minimum zones in the tropical oceans. Science 320, 655–658.

Stramma, L., Kieke, D., Rhein, M., Schott, F., Yashayaev, I., Koltermann, K.P., 2004. Deep water changes at the western boundary of the subpolar North Atlantic during 1996 to 2001. Deep-Sea Res. I 51, 1033–1056.

Sundby, S., Drinkwater, K., 2007. On the mechanisms behind salinity anomaly signals of the northern North Atlantic. Progr. Oceanogr. 73, 190–202.

Sutton, R.T., Jewson, S.P., Rowell, D.P., 2000. The elements of climate variability in the tropical Atlantic region. J. Clim. 13, 3261–3284.

Swift, J.H., Aagaard, K., Timokhov, L., Nikiforov, E.G., 2005. Long-term variability of Arctic Ocean Waters: Evidence from a reanalysis of the EWG data set. J. Geophys. Res. 110 C03012. doi:10.1029/2004JC002312.

Talley, L.D., 1996b. North Atlantic circulation and variability, reviewed for the CNLS conference. Physica. D 98, 625–646.

Talley, L.D., 2008. Freshwater transport estimates and the global overturning circulation: Shallow, deep and throughflow components. Progr. Oceanog. 78, 257–303. doi:10.1016/j.pocean.2008.05.001.

Thompson, D.W.J., Solomon, S., 2002. Interpretation of recent southern hemisphere climate change. Science 296, 895–899.

Thompson, D.W.J., Wallace, J.M., 1998. The Arctic- Oscillation signature in the wintertime geopotential height and temperature fields. Geophys. Res. Lett. 25, 1297–1300.

Thompson, D.W.J., Wallace, J.M., 2000. Annular modes in the extratropical circulation. Part I: Month-to-month variability. J. Clim. 13, 1000–1016.

Tourre, Y.M., White, W.B., 1995. ENSO Signals in global upper-ocean temperature. J. Phys. Oceanogr. 25, 1317–1332.

Tourre, Y.M., White, W.B., 1997. Evolution of the ENSO signal over the Indo-Pacific domain. J. Phys. Oceanogr. 27, 683–696.

Trenberth, K.E., Hurrell, J.W., 1994. Decadal atmosphere-ocean variations in the Pacific. Clim. Dyn. 9, 303–319.

Trenberth, K.E., Jones, P.D., Ambenje, P., Bojariu, R., Easterling, D., Klein Tank, A., Parker, D., Rahimzadeh, F., Renwick, J.A., Rusticucci, M., Soden, B., Zhai, P., 2007. Observations: Surface and Atmospheric Climate Change. In: Solomon, S., Qin, D., Manning, M., Chen, Z., Marquis, M., Averyt, K.B., Tignor, M., Miller, H.L. (Eds.), Climate Change 2007: The Physical Science Basis. Contribution of Working Group I to the Fourth Assessment Report of the Intergovernmental Panel Climate Change. Cambridge University Press, Cambridge, UK and New York.

Vellinga, M., Wood, R.A., 2002. Global climatic impacts of a collapse of the Atlantic thermohaline circulation. Climatic Change 43, 251–267.

Visbeck, M., 2002. The ocean's role in climate variability. Science 297, 2223–2224.

Visbeck, M., Chassignet, E.P., Curry, R.G., Delworth, T.L., Dickson, R.R., Krahmann, G., 2003. The ocean's response to North Atlantic Oscillation variability. In: The North Atlantic Oscillation: Climate significance and environmental impact. Geophys. Monogr. Ser. 134, 113–146.

Wang, C., 2002. Atlantic climate variability and its associated atmospheric circulation cells. J. Clim. 15, 1516–1536.

WCRP, 1998. CLIVAR Initial Implementation Plan. WCRP-103, WMO/TD No. 869, ICPO No. 14, 367 pp.

Webster, P.J., Magana, V.O., Palmer, T.N., Shukla, J., Tomas, R.A., Yanai, M., Yasunari, T., 1998. Monsoons: Processes, predictability, and the prospects for prediction. J. Geophys. Res. 103, 14451–14510.

Webster, P.J., Moore, A.M., Loschnigg, J.P., Leben, R.R., 1999. Coupled ocean-atmosphere dynamics in the Indian Ocean during 1997–98. Nature 401, 356–360.

Wong, A.P.S., Bindoff, N.L., Church, J.A., 2001. Freshwater and heat changes in the North and South Pacific Oceans between the 1960s and 1985–94. J. Clim. 14, 1613–1633.

Yashayaev, I., 2007. Hydrographic changes in the Labrador Sea, 1960–2005. Progr. Oceanogr. 73, 242–276.

Yuan, X., 2004. ENSO-related impacts on Antarctic sea ice: a synthesis of phenomenon and mechanisms. Antarct. Sci. 16, 415–425. doi:10/1017/S0954102004002238.

Zhang, R., Vallis, G.K., 2006. Impact of Great Salinity Anomalies on the low-frequency variability of the North Atlantic Climate. J. Clim. 19, 470–482.

Zhong, A., Hendon, H.H., Alves, O., 2005. Indian Ocean variability and its association with ENSO in a global coupled model. J. Clim. 18, 3634–3649.